



Cite this: *Chem. Soc. Rev.*, 2023, 52, 248

Received 6th September 2022

DOI: 10.1039/d2cs00762b

rsc.li/chem-soc-rev

# 4'-Fluoro-nucleosides and nucleotides: from nucleocidin to an emerging class of therapeutics

Phillip T. Lowe \* and David O'Hagan \*

The history and development of 4'-fluoro-nucleosides is discussed in this review. This is a class of nucleosides which have their origin in the discovery of the rare fluorine containing natural product nucleocidin. Nucleocidin contains a fluorine atom located at the 4'-position of its ribose ring. From its early isolation as an unexpected natural product, to its total synthesis and bioactivity assessment, nucleocidin has played a role in inspiring the exploration of 4'-fluoro-nucleosides as a privileged motif for nucleoside-based therapeutics.

## 1. Introduction

Organofluorine compounds constitute around 25% of all pharmaceuticals that have been licensed since the development of modern medicinal chemistry and that number is increasing for products in development.<sup>1</sup> The ratio is even higher, at around 30%, for organofluorines found in agrochemical products

including pesticides and herbicides.<sup>2,3</sup> The incorporation of fluorine has been weaponised to fine tune pharmacokinetic profiles and other performance indicators to the point where the bioactives industries rely on the fluorine as a tool for optimisation.<sup>1,4–7</sup> Thus, it is something of a paradox that nature has essentially ignored fluorine as an element in the biosynthesis of natural products, that myriad of compounds which are often characterised by their structural complexity, and which have largely evolved as bioactives to improve the fitness of the producing organism. Fluorinated natural products are exceedingly rare, to the point that new isolations attract significant

School of Chemistry and Biomedical Sciences Research Centre, University of St Andrews, North Haugh, St Andrews KY16 9ST, UK. E-mail: pl49@st-andrews.ac.uk, do1@st-andrews.ac.uk



Phillip T. Lowe

*Dr Phillip Lowe received an MChem degree at the University of Manchester and continued his postgraduate research at the Manchester Institute of Biotechnology, where he developed RNA-based gene expression tools capable of dynamic control of gene expression, for which he was awarded a PhD in Biological Chemistry. He is currently a Postdoctoral Research Fellow in the O'Hagan group at the University of St Andrews where his*

*research has focused on the biotechnological development of the fluorinase enzyme, elucidating the biosynthesis of fluorometabolites and the production of novel bio-based fluorochemicals.*



David O'Hagan

*Professor David O'Hagan studied for his first degree in chemistry at the University of Glasgow and then PhD at the University of Southampton. He carried out postdoctoral research at the Ohio State University before being appointed to a Lectureship at the University of Durham. At Durham he combined his interests in natural products biosynthesis with organo-fluorine chemistry and began a programme exploring the biosynthesis of the rare naturally occurring fluorine containing*

*compounds. In 2000 he moved to his current location at the University of St Andrews in Scotland where he is associated with both the School of Chemistry and the Centre for Biomolecular Sciences (BMS). At St Andrews his laboratory isolated the fluorinase, a native C–F bond forming enzyme and they have an active interest in exploring nucleocidin biosynthesis. Professor O'Hagan is the current President of the Organic Chemistry Community of the Royal Society of Chemistry.*



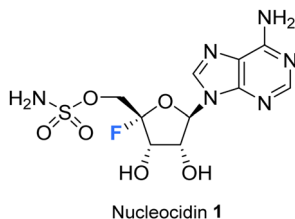


Fig. 1 Structure of nucleocidin.

interest. Fluoroacetate is the most common metabolite of this class having been identified widely in tropical and sub-tropical plants and in some bacteria. It has the obvious attribute of being exceedingly toxic and has presumably been harnessed by these organisms to fend off predators. Almost all the other fluorometabolites that have been identified so far are biosynthetically related to fluoroacetate and can be deduced to have arisen as products, branching from the same biosynthetic pathway. The only exception to this is nucleocidin 1 (Fig. 1), which was originally isolated from the actinomycete bacterium, *Streptomyces calvus*.<sup>8</sup>

Fluorination has been extensively utilised in medicinal chemistry to imbue desired characteristics on nucleoside and nucleotide analogues towards a wide range of applications. For instance, the incorporation of fluorine motifs within nucleobases, and structural analogues thereof, has been investigated as a tool to mechanistically probe nucleic acids and proteins.<sup>9–13</sup> Incorporation of fluorine within a non-canonical sugar motif of a nucleoside and a nucleotide has been used to generate analogues with tailored conformation and properties when incorporated into oligonucleotides and thus optimise potential biological applications.<sup>14–16</sup> Additionally, modification of the nucleic acid backbone using fluorinated PNA monomers has been successfully explored,<sup>17,18</sup> as has the development of selectively fluorinated nucleoside amidate prodrugs as antivirals.<sup>19,20</sup>

In pharmaceuticals research, nucleosides modified by selective fluorination on the ribose ring have proven to be a rich source of bioactives and a diversity of such compounds has been developed for a variety of applications, most prominently as antiviral agents.<sup>21–24</sup> Significant compounds of this class are illustrated in Fig. 2. Sofosbuvir 9 (anti Hep C virus) is a spectacular case in point and has been one of the most successful drugs of all time in commercial terms,<sup>25</sup> but there are many other therapeutics of this class such as Lodenosine 3 (FddA) now discontinued,<sup>26</sup> and Gemcitabine 4,<sup>27</sup> and Clofarabine 5<sup>28</sup> which are currently used as clinical chemotherapeutics. It is noteworthy however that in all of these cases the fluorine atom is located at either the 2' and 3' positions of the ribose ring and not the 4'-position found in nucleocidin 1.<sup>29</sup>

The utility of nucleosides incorporating a variety motifs at C4' of the ribose, such as azides and alkyl groups, have been quite widely studied.<sup>30,31</sup> It emerges that substituents incorporated at the C4' position become located along the backbone edge of a nucleic acid duplex when assembled into higher ordered structures, and modifications at this position avoid notable steric clashes.<sup>31,32</sup> Consequently, C4'-modified nucleosides have found a range of biomedical applications from oligomeric nucleotide therapeutics to antiviral agents.<sup>30,33,34</sup> It is notable however that nucleosides with fluorine at the 4' position of the ribose moiety have featured far less over the years, certainly relative to the abundance of analogues with fluorine at C2' and C3'. There are perhaps some obvious reasons for this. The chemistry required to introduce a C4' tertiary fluorine is particularly challenging and with the added complexity of controlling stereochemistry. Also, when fluorine is placed at C4' of the ribose, it is potentially labile as it has an anomeric relationship with the ether oxygen and becomes susceptible to fluoride ion elimination. This can be contrasted with the relative stability of fluorine at C2' and C3'. However, with these caveats, such compounds can be made stable and there have been recent

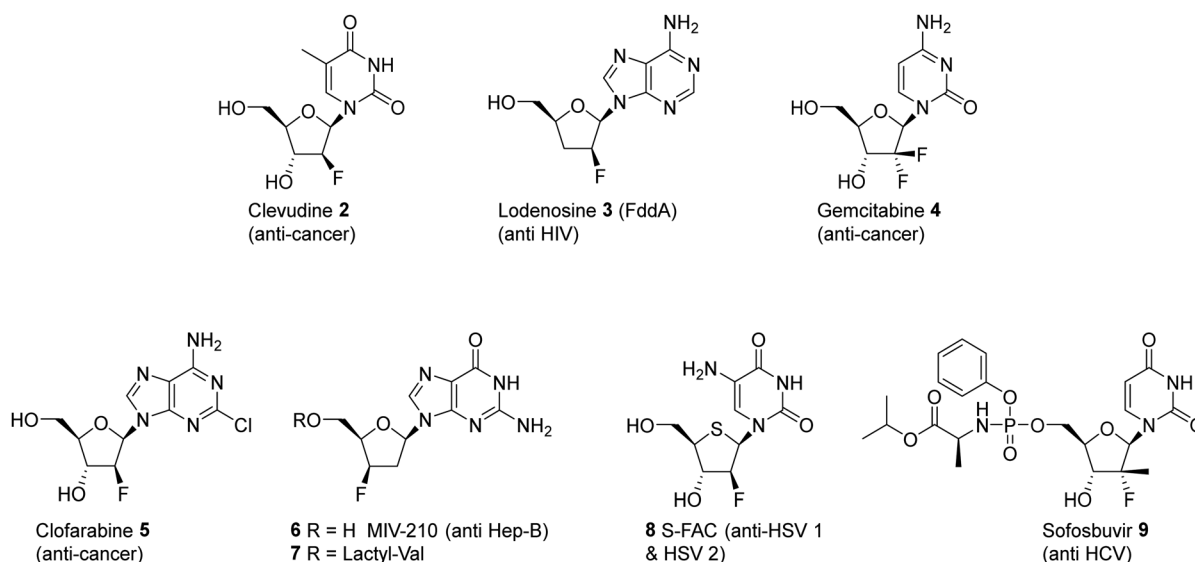


Fig. 2 Examples of clinically significant fluorinated nucleosides and their target applications.



disclosures in both the primary and patent literature outlining the preparation of synthetic 4'-fluoro-nucleosides in order to assess them as antivirals, and in that context there has been a particular focus on anti-hepatitis-C therapies.<sup>35,36</sup>

Nucleocidin **1** is the only fluorine containing nucleoside so far isolated from a natural source and it is an intriguing contradiction that the fluorine is located at C4', the chemically most challenging site relative to the more common C2' and C3' fluoro-nucleosides which have emerged from med-chem programmes.<sup>37</sup> This review aims to survey the literature to date on this class of nucleosides, highlighting recent developments in the identification of novel 4'-fluoro-nucleoside metabolites associated with nucleocidin production, as well as outlining progress in the synthesis and development of 4'-fluoro-nucleosides in chemical biology and as candidate antiviral agents among other biological applications.

## 2. Natural 4'-fluoro-nucleosides

### 2.1 Nucleocidin isolation and structural elucidation

Nucleocidin **1** was first isolated from the bacterium *Streptomyces calvus* in 1956, an actinomycete cultured from an Indian soil sample.<sup>8</sup> It took over a decade to establish that nucleocidin contained a fluorine atom and another decade before the correct 4'-fluoro-5'-O-sulfamyl adenosine structure was confirmed by total synthesis.

Initial attempts at structure elucidation by Waller *et al.* (1957) utilised a variety of chemical and spectroscopic techniques (IR, UV and chemical hydrolysis) and provided a promising yet incomplete structural for nucleocidin (Fig. 3).<sup>38</sup> Structure **11** was proposed with adenine bound to a carbohydrate moiety (specifically a 9-adenyl glycoside) and with a sulfamyl moiety attached. However, due to instrument limitations and inaccurate elemental analysis ( $C_{11}H_{16}N_6SO_8$ ), the presence of a fluorine was overlooked. Hydrolysis, chromatography and  $pK_a$  studies confirmed the hexavalent nature of the sulfur, and a sulfamyl group was proposed, however a complete structure was still not confirmed at this point.<sup>38</sup> At the time of publication few synthetic examples had been reported of esters of N-unsubstituted sulfamic acids,<sup>38</sup> and to date the existence of natural products containing a sulfamate group is rare.<sup>39,40</sup> Morton *et al.*, proposed a correct structure for nucleocidin in 1969 using  $^1H$ -NMR,  $^{19}F$ -NMR and mass spectrometry.<sup>37</sup> The advent of more powerful NMR spectrometers identified coupling constants between the C3'/H and C5'/H

methylene protons and fluorine and this, with accurate mass ( $C_{10}H_{18}N_6SO_6F$ ) determination and fragmentation, allowed deduction of the established structure as 9-(4-fluoro-5-O-sulfamoylpento-furanosyl)adenine (Fig. 3). This placed nucleocidin **1** among the exceedingly rare fluorine containing natural products and set it apart from fluoromethyl related structures such as fluoroacetate, as the only fluoro-nucleoside derivative.<sup>37</sup> The absolute D-configuration of the ribose sugar was subsequently confirmed with the total synthesis of nucleocidin **1**.<sup>41,42</sup>

### 2.2 Biological activity of nucleocidin

Nucleocidin **1** was soon recognised to have significant anti-trypanosomal activity.<sup>38</sup> Hewitt *et al.* revealed a remarkable activity against *T. equiperdum* in 1956,<sup>43</sup> reporting that it was considerably more potent than the structurally related antibiotic puromycin.<sup>44</sup> Subsequent assessments found it active against a number of trypanosoma species; in 1957 Tobie *et al.* found it to be highly effective against *T. congolense*, *T. equinum* and *T. gambiense* in mice and rats, at a dose of 0.15 mg per kg, although it was also demonstrated to display a significant toxicity.<sup>45</sup> In a study by Stephen *et al.*, in 1960 it was demonstrated to be active against *T. vivax* in West African Fulani zebu cattle at low concentrations (0.025 mg per kg), however relapses occurred within one month after treatment.<sup>46</sup> Nucleocidin was also found to be active in inhibiting the growth of several insect parasites such as *Leptomonas* and *C. fasciculata*, with a comparable potency to established trypanocides and leishmanicides.<sup>47</sup>

In terms of understanding nucleocidin's mode of action, Florini *et al.* in 1966 and later, Sherman *et al.*, in 1976, demonstrated a potent inhibition of protein synthesis. This occurred *in vivo* at doses much lower than that of other available antibiotics at the time,<sup>48,49</sup> although the demonstrated potency was considerably diminished in cell free systems.<sup>48</sup> At the molecular level, nucleocidin appears to inhibit translation and specifically the transfer of amino acids from tRNA's into the growing polypeptide chain at a stage subsequent to the formation of the aminoacyl-RNA. This is a consequence of an unusually slow but reversible formation of a co-complex between nucleocidin and the ribosome.<sup>48</sup>

The effect of nucleocidin on the fine structure of a monomorphic strain of *Trypanosoma rhodesiense* has also been examined by Williamson *et al.*<sup>50</sup> This study revealed that nucleocidin induced electron-lucent cytoplasmic clefts in the cytoplasm of *T. rhodesiense* which possessed a close relationship with the rough

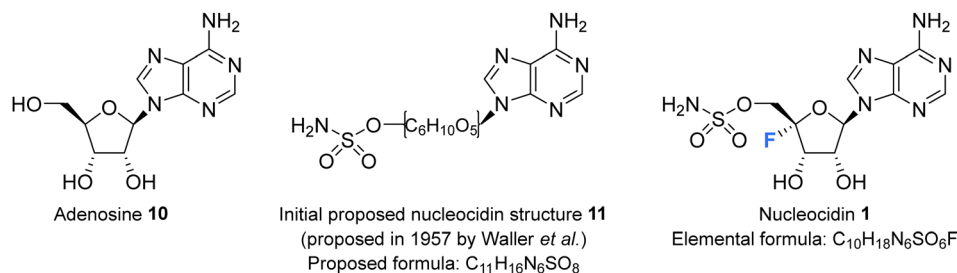


Fig. 3 Adenosine **10**, the initially proposed structure **11** for nucleocidin<sup>38</sup> and the corrected structure of nucleocidin **1** containing a C4'-fluorine.<sup>37</sup>



endoplasmic reticulum and also resulted in excessive lysosomal vacuolation. Also noted was nucleocidin's ability to provoke nucleolar fragmentation and segregation, an outcome which may be related to interference with RNA synthesis.<sup>50</sup>

Given its potency and palatability to animals, nucleocidin appeared at the outset to offer a promising treatment for trypanosomal infections, however as a broader trypanocidal and leishmanicidal activity was demonstrated, so too was its toxicity. Numerous investigations revealed high toxicity in mice ( $LD_{50}$  – injection:  $0.2 \text{ mg kg}^{-1}$ , oral:  $2 \text{ mg kg}^{-1}$ ), rabbits (lethal subcutaneous doses of  $5.0 \text{ mg kg}^{-1}$ ), rats (lethal injection:  $0.8 \text{ mg kg}^{-1}$ ) and most strikingly in young bovines (lethal –  $0.05 \text{ mg kg}^{-1}$ ) and thus any therapeutic promise was impeded by its high toxicity. This was exacerbated too by its lack of availability as it was not yet synthetically accessible, and titres were low from fermentation.<sup>43</sup>

### 2.3 Nucleocidin co-produced metabolites

The original strains of *S. calvus* deposited in public culture collections at the time of isolation subsequently lost their capacity to produce nucleocidin in culture. This hindered biosynthetic investigations as there were no available producing cultures. It was not until relatively recently that Zechel and Bechthold recognised from genome sequencing that the publicly available strain *S. calvus* ATCC 13382 associated with nucleocidin production was carrying a mutation in a *bldA* gene.<sup>51</sup> This gene codes for

the production of Leu-tRNA<sup>UUA</sup> which is required to translate leucine into selected proteins when instructed by the genome with the relatively rare TTA codon in some genes. Several genes implicated in nucleocidin biosynthesis utilise this codon and when the *bldA* mutation was corrected nucleocidin production became re-established in culture. This clearly indicated the importance of that particular codon usage for the incorporation of leucine into at least one of the biosynthetic enzymes for nucleocidin assembly.<sup>51,52</sup> The original industrial *S. calvus* T-3018 strain held by Wyeth and then Pfizer had retained an ability to produce nucleocidin and with these producing strains available there has been a renewed interest in exploring nucleocidin biosynthesis.<sup>53,54</sup> In particular, this has resulted in a deeper interrogation into the structures of minor fluorine containing metabolites co-produced with nucleocidin in *S. calvus*.

Fig. 4 indicates the current metabolite profile of nucleocidin and its related structures from *S. calvus*. Most notable are the recently identified 3'-glucosylated metabolites F-Met I 12 and F-Met II 13. These compounds become apparent by <sup>19</sup>F-NMR in extracts of *S. calvus* taken from the fermentation after a few days (days 5–6) but before nucleocidin production (day 8).<sup>55</sup> As nucleocidin 1 begins to accumulate both F-Met I 12 and F-Met II 13 disappear in supernatant extracts, giving some sense that they are biosynthetic precursors to the finally formed nucleocidin 1.<sup>55</sup>

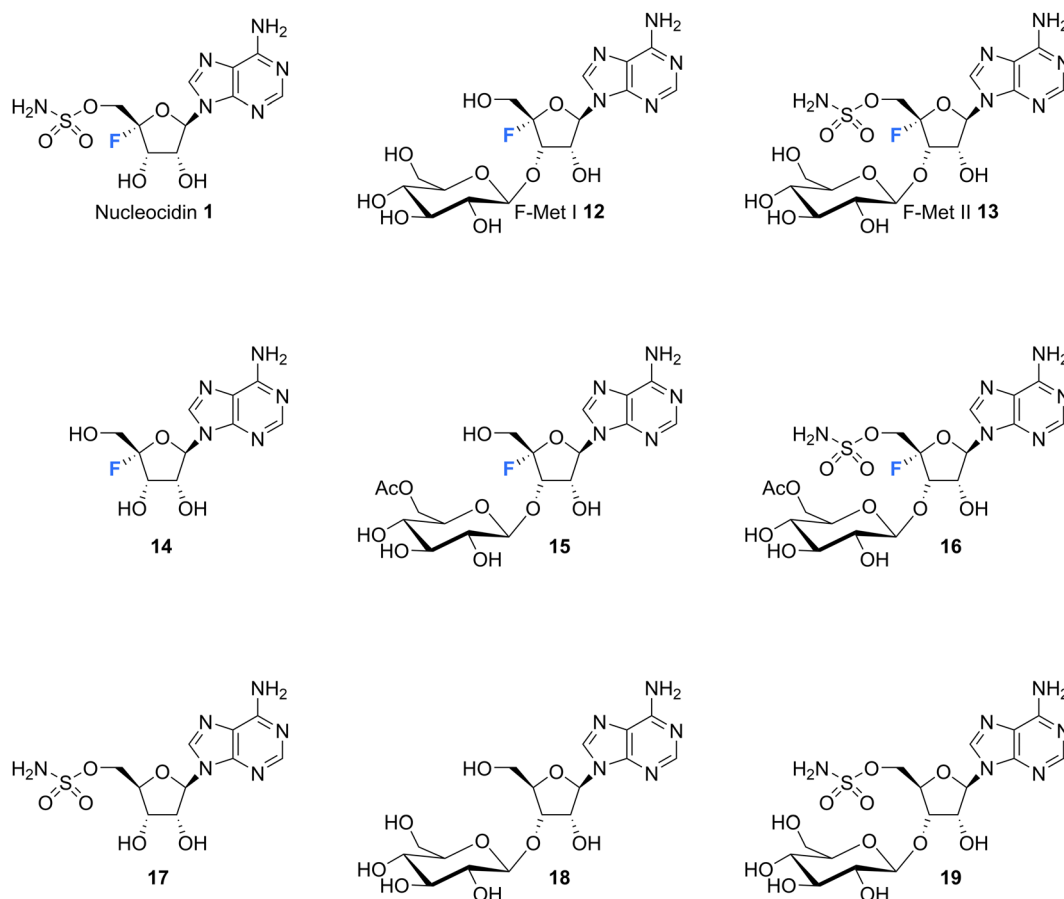


Fig. 4 Structures of co-produced metabolites with nucleocidin from *S. calvus* and also *S. vires* B-24331 and *S. aureorectus* B-24301.





Isolation and structure elucidation has established that F-Met I **12** and F-Met II **13** are both  $\beta$ -glucosylated on the 3'-OH of the ribose, which is a rare regiospecific glucosylation of nucleosides in metabolism. Genome mining identified a candidate glucosyl transferase gene (*nucGT*)<sup>55</sup> which, when over-expressed, was shown to efficiently  $\beta$ -glucosylate the 3'-hydroxyl of adenosine **10** and 5'-O-sulfamyl adenosine **17** in *in vitro* assays with uridine diphosphate glucose (UDP-glucose) as the glucose donor. Such an unusual regiochemistry indicates that this enzyme is responsible for the biosynthesis of F-Met I **12** and F-Met II **13**. Glucosylation is a general strategy used by microorganisms to export toxic metabolites extracellularly and this may be a means of removing toxic 4'-fluoro-nucleosides from the cell. The recent discovery of nucleocidin producers by genome comparisons revealed *Streptomyces vires* B-24331 and *Streptomyces aureorectus* B-24301 as close relatives to *S. calvus*, and these organisms produce greater titres of nucleocidin and its related derivatives. Two *O*-acetylated metabolites **15** and **16** (see Fig. 4) were identified as minor metabolites from *S. vires*, and a glycosyl-*O*-acetyltransferase in the genome appears to be responsible for their production from F-Met I **12** and F-Met II **13** respectively.<sup>39</sup> These acetylated metabolites are not obvious in *S. calvus* and they, along with their F-Met I **12** and F-Met II **13** precursors, appear to be metabolites of the first formed fluorometabolite, the nature of which is not clear at present. Another recent nucleocidin related metabolite is 4'-fluoroadenosine **14**. This was identified in *S. vires* as a minor metabolite which appears very late in the batch fermentation cycle, after nucleocidin **1** production.<sup>56</sup> This timing leaves open the prospect that 4'-fluoroadenosine **14** is a metabolite rather than a biosynthetic precursor to nucleocidin, although this remains to be determined.

Intriguingly, a selection of nucleocidin analogues without a fluorine have been identified in wild type cultures of *S. calvus*.<sup>57</sup> Defluoro-nucleocidin **17** as well as the corresponding  $\beta$ -glucosylated analogues **18** and **19** were recently isolated and their structures established relative to synthetic and enzymatically prepared reference compounds. These defluorohydra-analogues are present at levels between 10–50% relative to their fluorinated counterparts. This metabolite profile suggests that the biosynthetic assembly of the sulfamyl moiety of nucleocidin appears to be entirely independent of the fluorination event, developing adenosines that are electively fluorinated or not at C4'. *In vitro* enzyme assays have demonstrated too that both classes of adenosines (fluorinated and not) are also substrates of the  $\beta$ -glucosylation enzyme Nuc-GT.<sup>55,57</sup> There is evidence too from gene knockouts that sulfamylation and fluorination are independent processes.<sup>39,54</sup>

### 3. Conformation of the 4'-fluororibose ring

Selective fluorination of ribonucleosides, and particularly deoxyfluorination at 2'C or 3'C of the ribose ring, is well known to influence ribose ring pucker in a predictable but opposite manner. In solution the ribose ring equilibrates between energy minima that approximate North and South ring conformations,

in a dynamic pseudo-rotation process.<sup>58,59</sup> The North ring conformation has C-3' carbon 'up' and *endo* relative to the C2' carbon, which is 'down' and *exo*. The South conformation has the opposite arrangement, with C3' carbon down and C2' carbon up as illustrated in the inset in Fig. 5.

Vicinal H1'-H2' coupling constants from NMR experiments in solution can be used as a proxy to distinguish North-type from South-type biased conformations. A value close to  $^3J_{\text{HH}} \sim 0$  Hz for the H1'-H2' vicinal coupling, represents a dihedral angle of 90° and is indicative of a pure North type conformation, whereas a vicinal H1'-H2' value of  $^3J_{\text{HH}} \sim 8$  Hz represents a dihedral angle approaching 180° and is indicative of a pure South type conformation.<sup>58,59</sup> Of course, experimental values represent an average of all population contributions in the pseudorotation interconversion.

For 2'-fluororibose several studies have concluded a predominant North-type conformation in solution.<sup>60</sup> This conformation accommodates an anti-periplanar arrangement between the 2'-C-F bond and the vicinal 3'-C-H bond, and thus a stabilising hyperconjugative interaction, typical of the classical *gauche* effect. Conversely for 3'-fluororibose systems a South-type conformation predominates.<sup>61,62</sup> This accommodates a stabilising hyperconjugative interaction between the 2'-C-H bond which can arrange antiperiplanar to the 3'-C-F bond.

For those examples studied so far, when fluorine is placed at C4' of the ribose in a nucleoside, then the North-type conformation dominates. The vicinal H1'-H2' coupling constants found in nucleocidin (1.9 Hz),<sup>42,63</sup> F-Met-I **12** (2.0 Hz),<sup>55</sup> F-Met-II **13** (0.9 Hz)<sup>55</sup> and 4'-fluoro-adenosine (2.9 Hz)<sup>56</sup> lie in the  $^3J_{\text{FH}} = 0.9$ –2.9 Hz range, suggesting only between  $\sim 10$ –30% of South-type conformer contributions. This is supported too by the vicinal 4'-F-3'H coupling constants which lie consistently between  $^3J_{\text{FH}} = 16$ –18 Hz for 4'-fluoro-adenosine **14**, nucleocidin **1** and metabolites F-Met-I **12** and F-Met II **13**, and the value equates to an antiperiplanar relationship between the C-F bond and the vicinal 3'-C-H bond. This preference is further reinforced when a fluorine is placed at C-2' in the case of 2',4'-difluoro-dideoxy ribose nucleotides.<sup>64</sup> In this case the vicinal H1'-H2' coupling constant equals  $^3J_{\text{HH}} = 0$  Hz, consistent with 100% North-type conformation, and the vicinal 4'-F-3'H coupling constant increases to  $^3J_{\text{FH}} = 21$  Hz further reinforcing an anti-periplanar arrangement between fluorine and the 3' hydrogen and the North-type conformer. Within this series a conformational analysis<sup>65</sup> of 4'-fluoro-2'-deoxythymidine by NMR also concluded a North-type conformation both as the free nucleotide with a vicinal H1'-H2' coupling of  $^3J_{\text{HH}} = 2.7$  Hz and assembled into an oligodeoxynucleoside. As the free nucleotide only 3% of the South-type conformation contributed, whereas within the oligodeoxynucleoside this increased to 37%, suggesting that the tertiary and quarternary structures were beginning to override the preferred stereoelectronic preferences of the isolated nucleotide, but again the North-type conformer predominated.

Finally, a study<sup>66</sup> on 3',4'-difluoro-3-deoxyadenosine concluded a North-type preference for this nucleoside. Notably this overturns the South-type preference of 3'-fluoro-deoxynucleotides, and thus introduction of a fluorine at the 4' position appears to dictate the



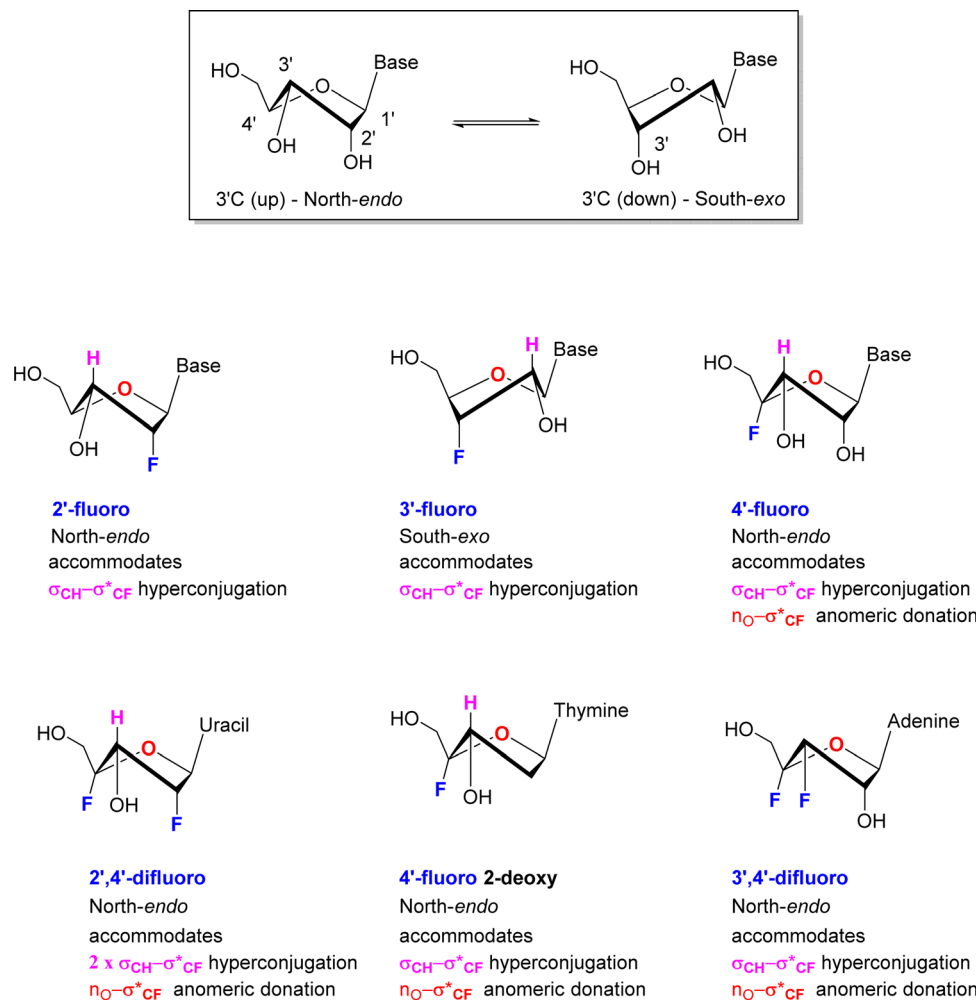


Fig. 5 Predominant sugar conformations of deoxyfluororibose nucleosides.

bias in favour of North-type. The clear predisposition to a North-type conformation for 4'-fluoro-nucleotides has an obvious origin in accommodating an anomeric type interaction between a ring oxygen lone pair and the pseudo axial C-F bond and given the observation that placing a fluorine at 3'-deoxyfluoro ribose switches the conformational bias, suggests that this anomeric interaction is more dominant, and overrides any  $\sigma_{\text{CH}}-\sigma^*_{\text{CF}}$  hyperconjugative interactions between antiperiplanar hydrogens and the C3'-fluorine.

## 4. Inhibition of RNA polymerases induced by 4'-fluoro-nucleotides

The predominant antiviral mode of action for most of the 4'-fluoro-nucleosides discussed in this review occurs *via* inhibition of viral RNA polymerases, and this necessitates that the 4'-fluoro-nucleosides (or their corresponding prodrug) are substrates for cellular kinases so that the 5'-triphosphates derivatives are formed *in vivo*. This manner of inhibition has been demonstrated *in vitro* for example by Wang *et al.*,<sup>35</sup> whereby the incorporation of a 4'-fluoro-nucleoside triphosphate into a growing RNA chain by a viral RNA polymerase results in

transcriptional stalling and the termination of chain elongation (Fig. 6). This mode of termination is presumably a consequence of the conformational North-type puckering of the 4'-fluoro-ribose, and the resulting interference this has upon the incorporation of subsequent nucleoside triphosphates (NTPs).

## 5. Preparation of 4'-fluoro-nucleosides and nucleotides

### 5.1 Total syntheses of nucleocidin 1

The first synthesis of nucleocidin **1**, was reported as a 'preliminary account' by Jenkins *et al.* in 1971<sup>67</sup> and is summarised in Scheme 1. A more complete account of this route was reported in 1976.<sup>42</sup> The report is of contemporary significance as it remains the most popular method for the synthesis of 4'-C-fluoro-nucleosides. The strategy centred on the introduction of the 4'-fluoro moiety to a protected 4',5'-dehydro-adenosine derivative, using an appropriate fluorinating pseudohalogen, in this instance iodine fluoride (Scheme 1).

The synthesis began with mesylation of *N*<sup>6</sup>-benzoyl-2',3'-O-isopropylidene-adenosine **20** and then a base induced elimination



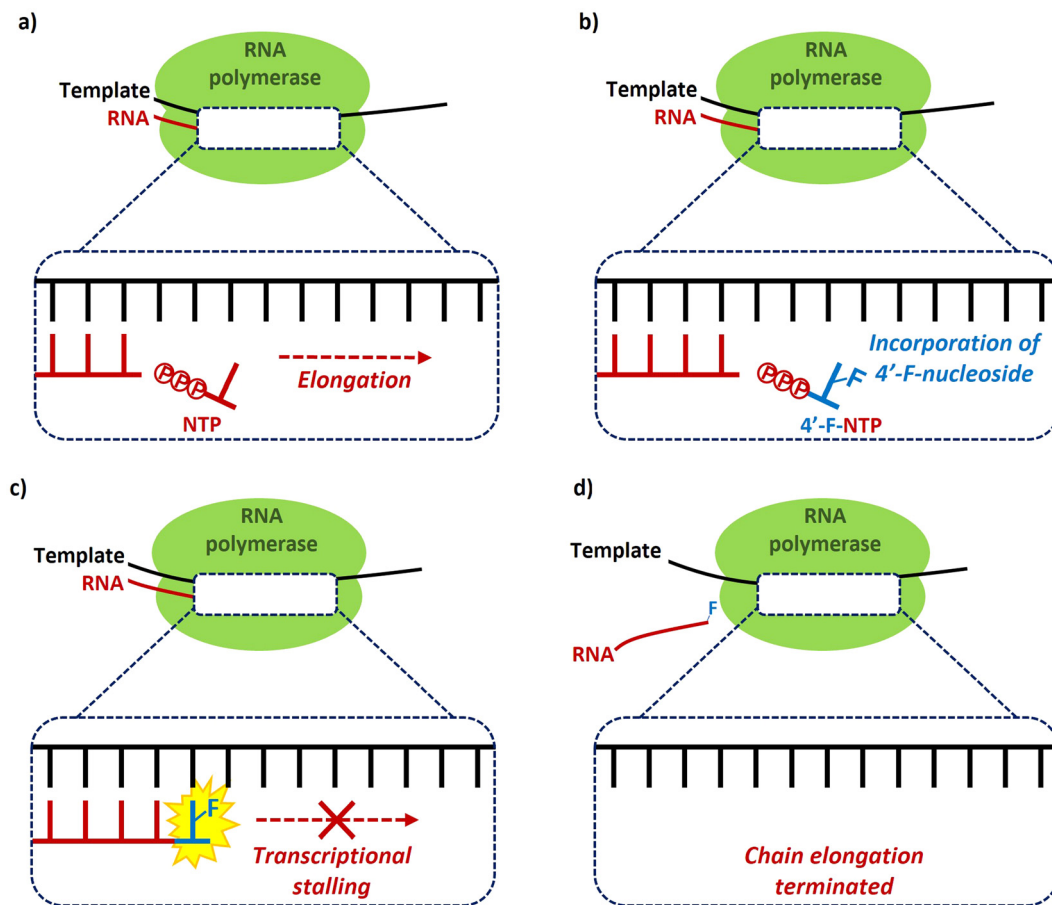


Fig. 6 Chain termination mechanism of inhibition of RNA polymerases by 4'-fluoro-nucleoside triphosphates, as exemplified by Wang *et al.*<sup>35</sup>

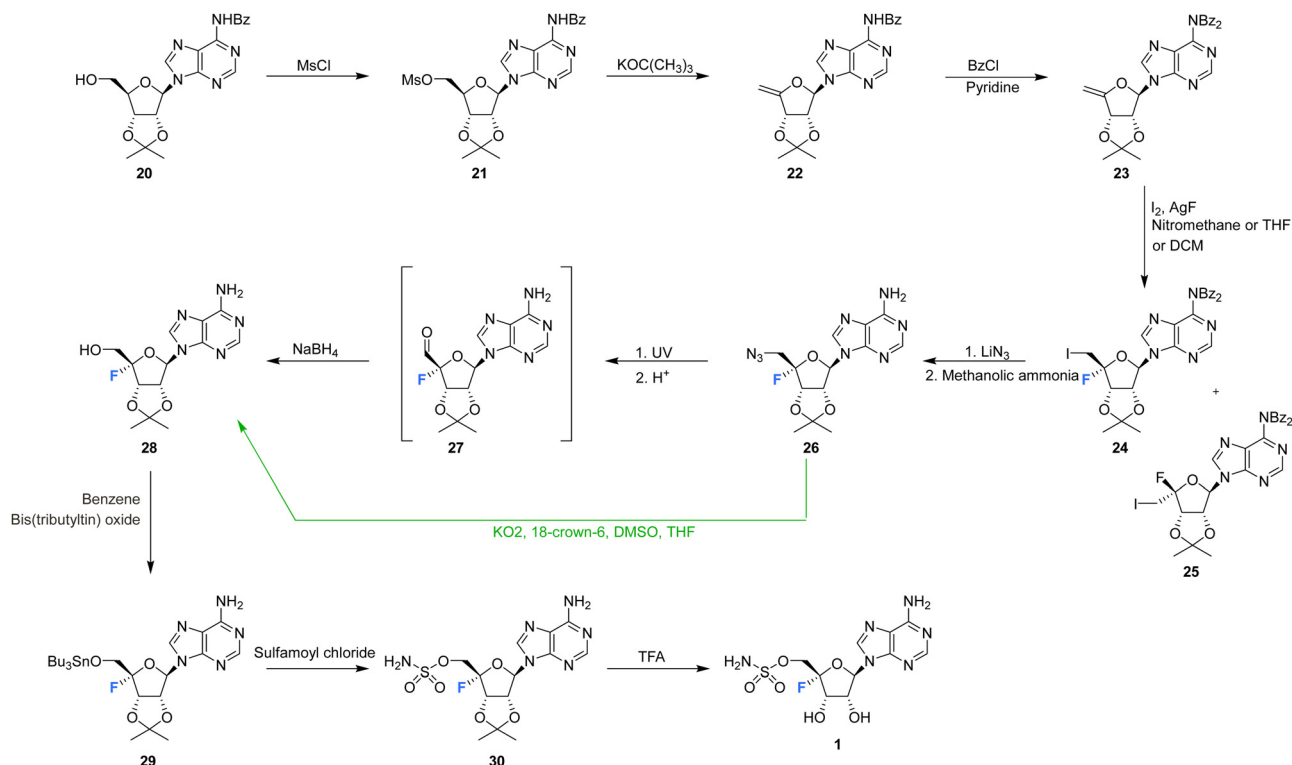
to generate the exocyclic enol ether **22**. Further benzoyl protection of the adenine ring was followed by iodo-fluorination of **23** using iodine and silver fluoride. This generated an epimeric mixture of 5'-deoxy-4'-fluoro-5'-iodonucleosides **24** and **25**, in a ratio which varied markedly depending on the reaction conditions.<sup>42,63</sup> Isomer **24** was separated by chromatography and was then progressed by nucleophilic substitution with lithium azide. Azide was one of the few nucleophiles capable of displacing this primary iodide and the presence of the  $\beta$ -fluorine appears to suppress such substitution reactions. Debenzoylation of the adenine was followed by conversion of the 5'-azide of **26** to alcohol **28** under UV irradiation, and *via* an intermediate aldehyde which was directly reduced using borohydride. Finally, installation of the sulfamyl group and removal of the ribose acetal afforded nucleocidin **1**. In 1993 Maguire *et al.* improved this general route (Scheme 1, green arrow), most notably by addressing the epimer ratio of **24**, which improved after slow addition of iodine and also using potassium superoxide in the conversion of azide **26** to alcohol **28**, circumventing the capricious photolytic conversion.<sup>63</sup>

## 5.2 4'-Fluoro-adenosines

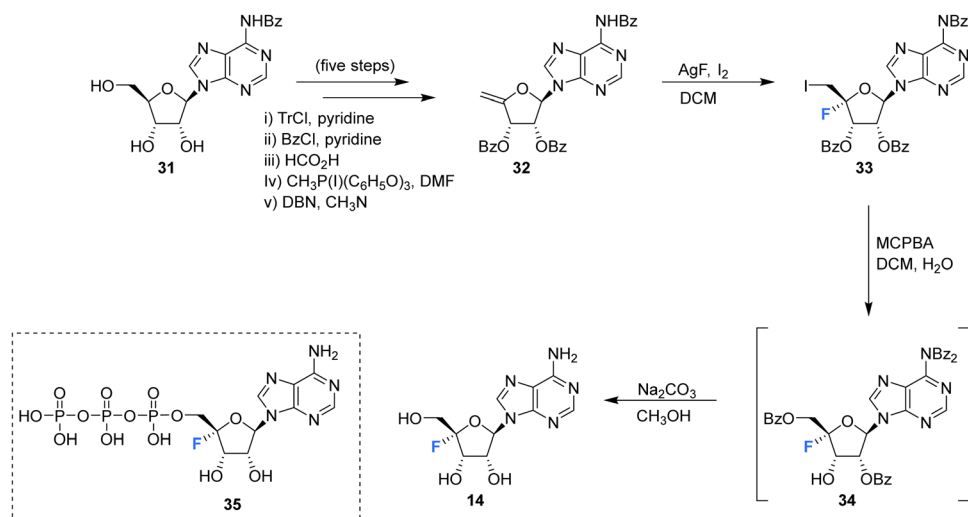
The first synthesis of 4'-fluoro-adenosine **14** was reported in 1995 by Guillerm *et al.*,<sup>68</sup> (Scheme 2) in a study to investigate whether it would function as an inhibitor of the antiviral target

*S*-adenosyl-L-homocysteine (AdoHcy) hydrolase. After a five step protocol to *N*<sup>6</sup>-benzoyl-9-(5-deoxy-2,3-*O*-dibenzoyl- $\beta$ -D-erythro-pent-4-enofuranosyl)adenine **32**, the fluorine was introduced using IF following a similar approach to the original total synthesis of nucleocidin. This generated the desired iodo-fluoro epimer **33**, although only in moderate yield. Conversion of the primary iodine to an alcohol was achieved with mCPBA and was followed by a global deprotection using sodium carbonate in methanol to generate **14**. 4'-Fluoro-adenosine **14** was found to be stable in both methanol (CD<sub>3</sub>OD, no decomposition) and buffered aqueous solutions (5% decomposition over a period of 4 d),<sup>68,70</sup> although it was observed to decompose rapidly in water (D<sub>2</sub>O, 80% in 1 day). 4'-Fluoro-adenosine **14** was shown to impart a time dependent loss of AdoHcy hydrolase activity ( $K_{\text{inact}} = 0.24 \text{ min}^{-1}$  and  $K_i = 166 \text{ }\mu\text{M}$ ), although with a significantly lower affinity for the enzyme (100 fold) than adenosine. This was attributed to the C3' *endo* geometry of the ribosyl moiety imposed by the 4'-C fluorine substituent.<sup>68</sup> Guillerm *et al.* proposed a "cofactor depletion mechanism" of inactivation of AdoHcy hydrolase by 4'-fluoro-adenosine **14**.<sup>68</sup> The 4'-fluoro-adenosine-5'-*O*-triphosphate **35** was acquired using established methods<sup>71</sup> by Mayes *et al.*<sup>69</sup> and was assayed for inhibitory activity against purified HCV polymerase where it was demonstrated to possess inhibitory activity with an  $\text{IC}_{50} > 10 \text{ }\mu\text{M}$ .<sup>69</sup>





Scheme 1 First total synthesis of nucleocidin **1**.<sup>42,67</sup> (distinct strategic deviations developed by Maguire *et al.*<sup>63</sup> are shown in green).



Scheme 2 Synthesis of 4'-fluoro-adenosine **14** as described by Guillermin *et al.*<sup>68</sup> and structure of 5'-O-triphosphate **35** synthesised by Mayes *et al.*<sup>69</sup>

The synthesis and biological evaluation of 4'-fluoro-adenosine-glycerodiphosphate **43** has been reported in the patent literature by Xu *et al.*<sup>72</sup> Protected adenosine derivative **36** was acquired as a mixture of isomers in five steps from **31** as illustrated in Scheme 3. Isomers **36** were then processed to the monophosphate **39** after treatment with methanolic ammonia and H<sub>2</sub>. The resultant monophosphate isomers **39** were coupled to morpholine using DCC to generate the morpholinophosphonate **40**. Subsequent coupling of **40** with protected glycerophosphate **41**, followed by TFA deprotection generated **43** as a single isomer after

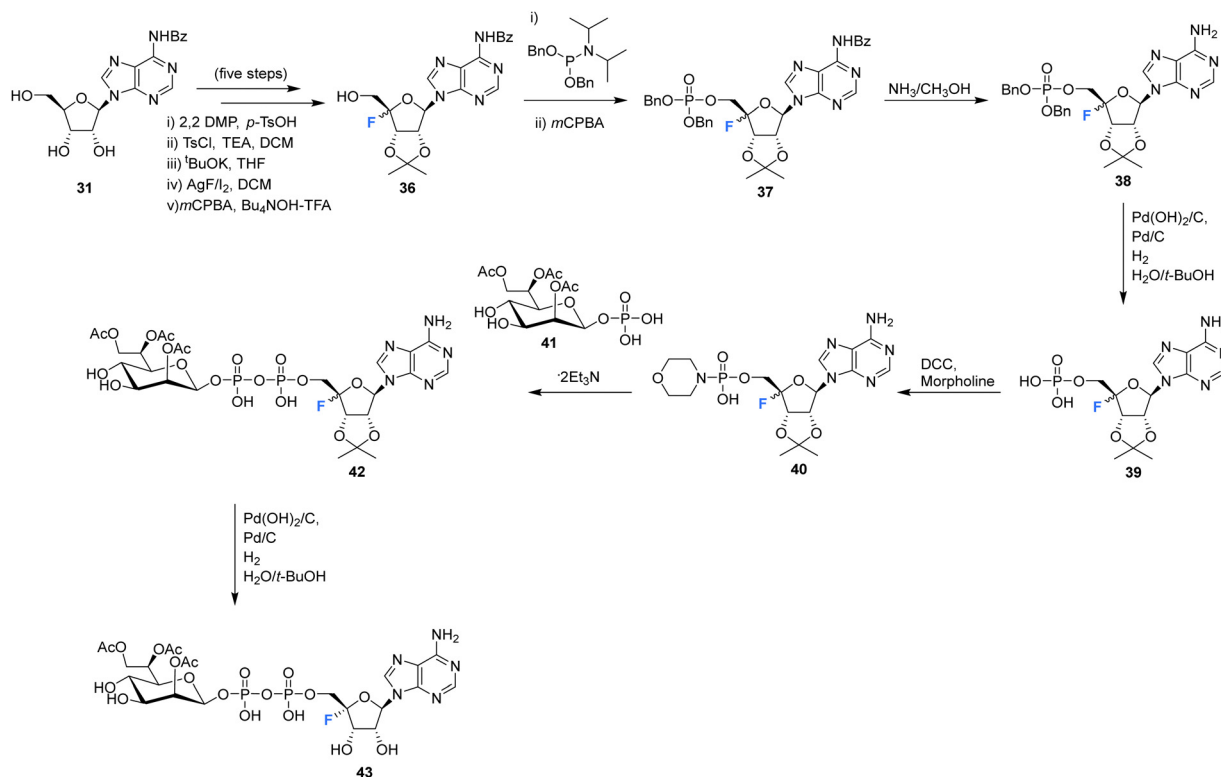
HPLC purification. Both 4'-fluoro-adenosine-glycerodiphosphate **43** and precursor **42** were assessed in tissue culture media of HEK293 cells and were shown to act as agonists for alpha protein kinase 1 (ALPK1) *in vitro*. Alpha protein kinase 1 plays an important role in the immune response and modulation of ALPK1 activity is a desired strategy for treating some cancers.

### 5.3 4'-Fluoro-uridines and cytidines

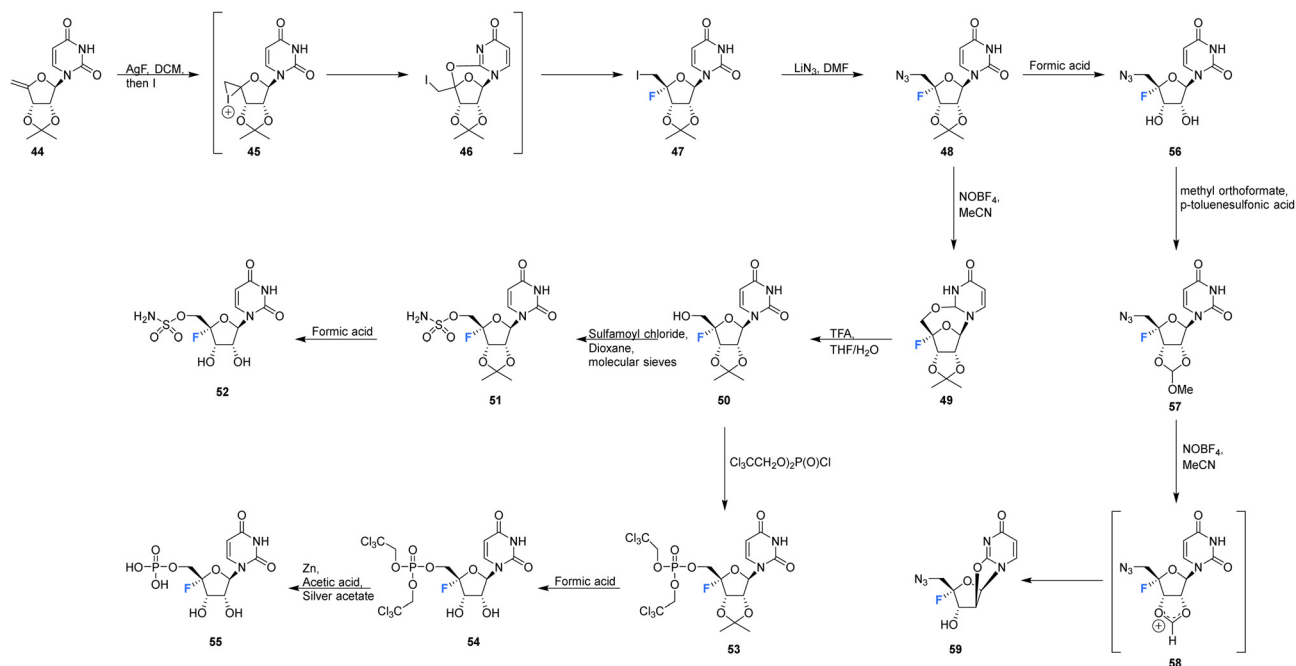
Owen *et al.* described the synthesis of 4'-fluoro-uridines **52**, **55** and **59** in 1976, see Scheme 4.<sup>73</sup> Experience with the introduction







Scheme 3 Synthesis of 4'-fluoro-adenosine-glycerodiphosphate **43** described by Xu *et al.*<sup>72</sup>



Scheme 4 Synthesis of 4'-fluoro-uridines **52**, **55** and **59** described by Owen *et al.*<sup>73</sup>

of substituents at C4' of the ribose ring in related systems suggested a 2',3'-cyclic carbonate to enable the correct stereochemical outcome from the addition of iodinefluoride to **44**. With this in mind, (5-deoxy-2,3-*O*-isopropylidene-β-D-erythro-pent-4-enofuranosyl)uracil **44** was subjected to a gradual treatment with

iodine in the presence of silver fluoride. This generated 5'-deoxy-4'-fluoro-5'-iodo-2',3'-*O*-isopropylideneuridine **47** as a single isomer. The remarkable stereoselectivity suggested anchimeric assistance from the uracil carbonyl occluding the top face of the ribose. Displacement of the relatively resistant 5'-iodo substituent with



azide required “forcing conditions” (lithium azide in DMF) to yield **48**, which was then treated with nitrosyl tetrafluoroborate to give  $O^2,5'$ -cyclonucleoside **49**. The lability of  $O^2,5'$ -anhydro-4'-fluoro-2',3'- $O$ -isopropylideneuridine **49** to undergo acidic hydrolysis was then exploited to afford alcohol **50**. Introduction of the sulfamoyl group to generate **51** was achieved by treatment with sulfamoyl chloride, and this was followed with isopropylidene deprotection using formic acid. Deprotection was accompanied by significant glycosidic cleavage, although preparative TLC allowed isolation of 4'-fluoro-5'-deoxy- $O$ -sulfamoyluridine **52** in a reasonable yield. **52** was found to exhibit considerably reduced antibacterial and cytotoxic properties when compared nucleocidin **1**. The electron withdrawing nature of the 5'- $O$ -sulfamoyl group seems to impart a favourable stability to nucleocidin, suppressing 4'-fluoride elimination. Similarly, the phosphate ester **55** was investigated as an alternative stabilising electron withdrawing substituent. Accordingly **50** was reacted with bis(2,2,2-trichloroethyl)phosphoric acid to generate phosphate **53** and then treatment with formic acid gave diol **54**. Finally, **55** was prepared after treatment of **54** with zinc in acetic acid and with catalytic silver acetate. The stability of these 4'-fluoro-uridine derivatives is strongly dependent on the nature of substituents attached to the 2',3'- and 5'-ribose hydroxyl groups with the protecting groups in **51**, **53**, and **57**, rendering the compounds more resistant to fluoride elimination, however removal of these substituents generated far less stable compounds. Phosphate ester **53** was found to be susceptible to alkaline hydrolysis (much more so than isopropylideneuridine **50**), although it was more stable in acidic conditions. The 5'-azido derivative **48** was sufficiently stable to allow a synthesis of 5'-azido-5'-deoxy-4'-fluoro-uridine **56**, and this was then used to access 2',3'- $O$ -methoxymethylene **57**. A treatment with nitrosyl tetrafluoroborate unexpectedly afforded  $O^2,2'$ -cyclo,4'-fluoronucleoside **59** in a process proceeding through an oxocarbenium ion.

Ivanov *et al.*, reported the synthesis of 4'-fluoro-uridine,5'- $O$ -triphosphate **68**, and investigated its efficacy against the hepatitis C virus, see Scheme 5.<sup>71</sup> The target **68** was prepared from 4'-fluoro-2',3'- $O$ -isopropylideneuridine **50**, itself prepared from **44** in a 4-step protocol involving fluorination ( $AgF/I_2$ ), azidation ( $NaN_3$ ), treatment with nitrosyl tetrafluoroborate and then hydrolysis to introduce the 5'-OH by a modification of the general method of Owen *et al.*<sup>73</sup> Product **50** was then coupled with the tris-triazolide of phosphoric acid to generate **67**, and then deprotection with formic acid gave 5'-monophosphate **55**. Activation of **55** with carbonyldiimidazole and then reaction with the *tert*-butylammonium salt of pyrophosphoric acid generated **68**, although the process was reported to be rather inefficient. The stability of 4'-fluoro-uridine,5'- $O$ -monophosphate **55** and triphosphate **68** were assayed in PBS buffer at 37 °C, and this revealed the formation of uracil with a half-life of approximately 18 h for both compounds, although both could be stored at -20 °C without degradation.

4'-Fluoro-uridine,5'- $O$ -triphosphate **68** was assayed as a potential inhibitor of two key hepatitis-C viral enzymes: Nucleoside triphosphate (NTP)-dependent RNA polymerase (NS5B) and NTP dependent NTPase/helicase (NS3). In the event **68** proved to be an effective inhibitor of the polymerase with an

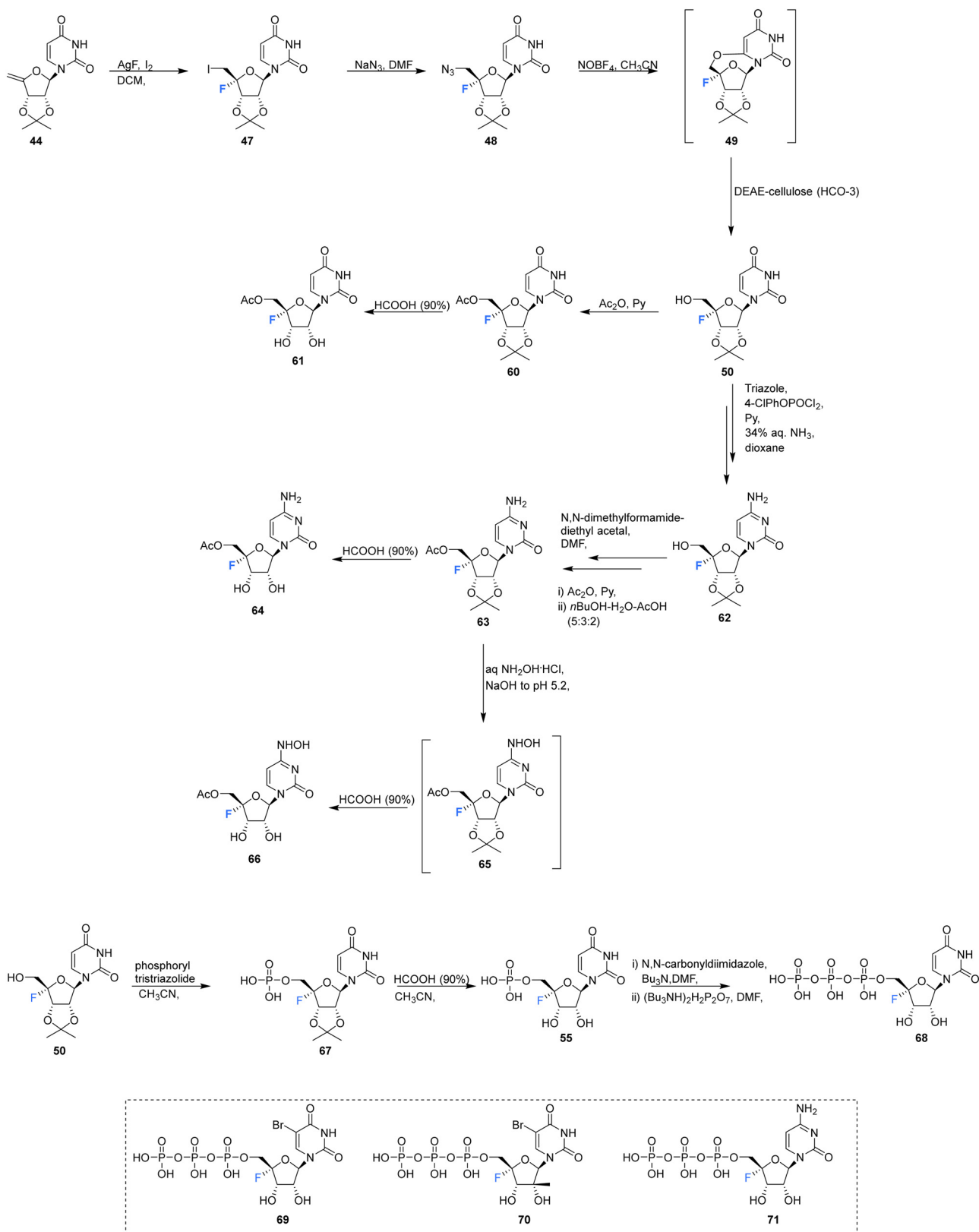
$IC_{50}$  of 2  $\mu M$ .<sup>71</sup> It was accepted as a substrate of the helicase but did not display any inhibition. Interestingly **68** acted as a substitute for ATP in its capacity as an allosteric activator of the helicase, but it was a significantly weaker binder than ATP.<sup>71</sup> Triphosphates **69–71** were also assayed against purified HCV polymerase by Mayes *et al.*<sup>69</sup> **71** displayed an  $IC_{50}$  between 250 nM–1  $\mu M$ , whereas **69** and **70** both displayed  $IC_{50}$ 's between 1–10  $\mu M$ .<sup>69</sup>

The acetyl derivatives **61**, **64** and **66** were synthesised from 4'-fluoro-2',3'- $O$ -isopropylideneuridine **50**. Each was found to be more stable than their non-acylated derivative. Acetylation of **50** with acetic anhydride in pyridine, followed by deprotection with formic acid, afforded acetylated 4'-fluoro-uridine **61**. Protected **50** was converted to its triazole, followed by aminolysis and then the same acetylation/deprotection treatment to generate acetylated 4'-fluoro-cytidine **64**. 4'-Fluoro-5'- $O$ -acetyl-2',3'- $O$ -isopropylideneuridine **63** was subjected to aqueous hydroxylamine solution to generate **65**, which was deprotected with formic acid, giving 4'-fluoro- $N^4$ -hydroxycytidine **66**. The ease at which 5'- $O$ -acetate is hydrolyzed by cell esterases allowed **61**, **64** and **66** to be assayed in cell cultures as prodrugs for their non-acylated counterparts. Antiviral activity can then be introduced through *in vivo* transformation to their triphosphate and then the anticipated inhibition of HCV RNA-dependent RNA polymerase. However in this study, no cytotoxic effects were observed in human hepatocyte Huh7 cell cultures (up to a concentration of 500  $\mu M$ ).<sup>71</sup>

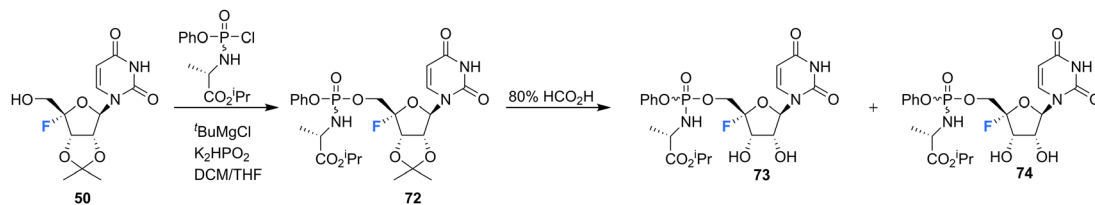
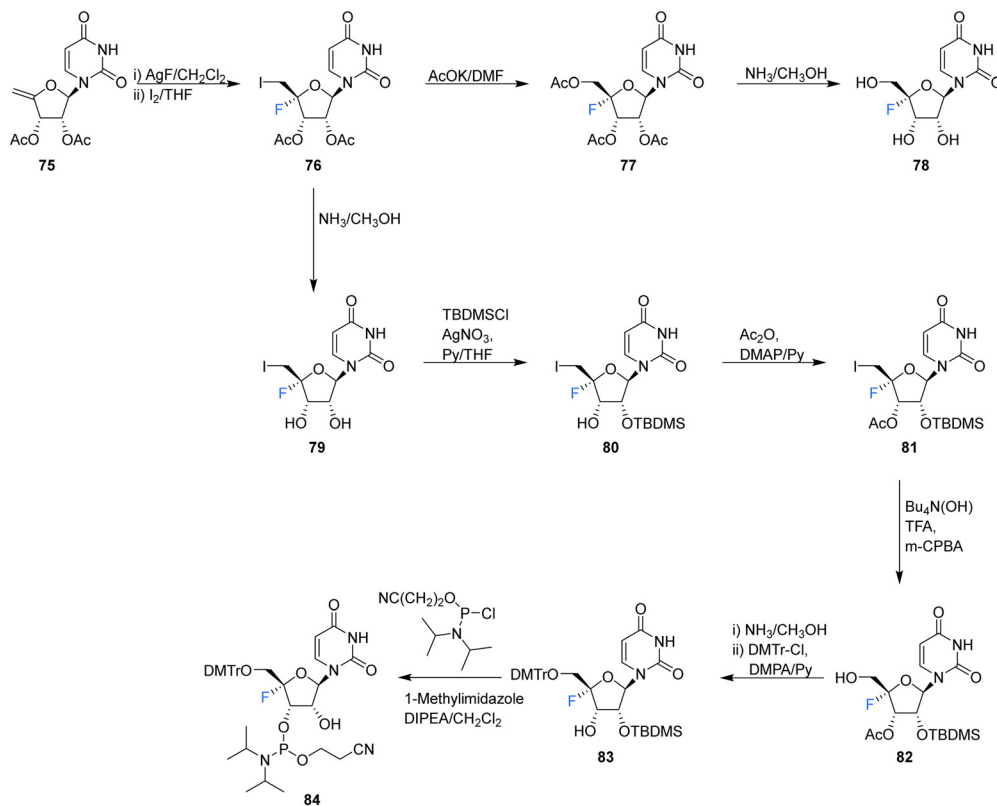
The synthesis of 4'-fluoro-uridine prodrugs **73** and **74** have been reported in the patent literature by Mayes *et al.*<sup>69</sup> 5'-Deoxy-4'-fluoro-5'-iodo-2',3'- $O$ -isopropylideneuridine **50** was generated using conventional methodology and was then converted with the appropriate chlorophosphoramidate followed by treatment with formic acid, as illustrated in Scheme 6. This afforded phosphoramidate diastereomers **73** and **74**, which could be separated by semi-prep HPLC, Scheme 6. Prodrugs **73** and **74** were assayed for HCV replicon activity and cytotoxicity. Diastereoisomers **73** and **74** both displayed  $CC_{50}$  values within the range of 1–10  $\mu M$ , with **73** possessing higher  $EC_{50}$  value (> 10  $\mu M$ ) than **74** (with the range of 1–10  $\mu M$ ). The pharmacokinetics of these prodrugs were studied, with the active nucleoside triphosphate for each compound measure by LC-MS/MS. Both **73** and **74** were found to readily accumulate in mouse liver samples.<sup>69</sup>

Recently, Li *et al.*, sought to investigate the use of 4'-fluoro-ribonucleosides as <sup>19</sup>F NMR probes in studies aiming to elucidate the structure and function of 4'-F-modified RNA.<sup>74</sup> With this in mind, the synthesis of phosphoramidite derivative **84** (along with 4'-fluoro-uridine **78**) was pursued (Scheme 7). The approach used a similar strategy to that of Owen *et al.*<sup>73</sup> with iodofluorination of 4',5'-dehydrouridine **75**. The desired 4'-fluoro-uridine **78** was obtained through displacement of the 5'-iodine by acetate, followed by deprotection of **77** with methanolic ammonia, although the general instability of **78** did not allow this route to progress further. Inspired by the inferred stability after modification at the 3'-OH of the nucleocidin co-metabolite F-Met II **13**, a step wise protection strategy was envisaged. Selective silylation of the 2'-OH using TBDMSCL,





Scheme 5 Synthesis of 4'-fluoro-uridine analogue **61**, 4'-fluoro-cytidine analogue **64**, 4'-fluoro- $N^4$ -hydroxycytidine **66**, 5'-O-triphosphate **68** described by Ivanov *et al.*<sup>71</sup> and structures of 5'-O-triphosphate **69–71** synthesised by Mayes *et al.*<sup>69</sup>

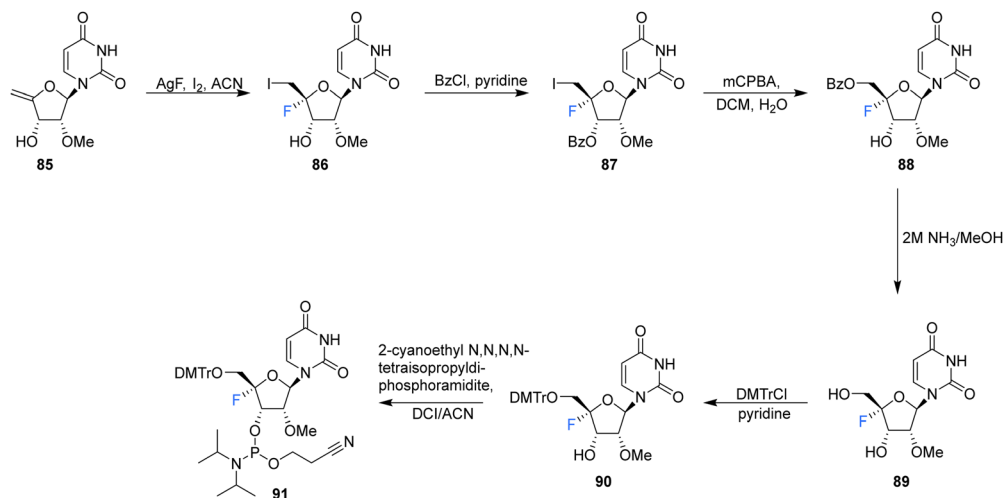
Scheme 6 Synthesis of 4'-fluoro-uridine prodrugs **73** and **74** described by Mayes *et al.*<sup>69</sup>Scheme 7 Synthesis of 4'-fluoro-uridine **78** and phosphoramidite derivative **84** as described by Li *et al.*<sup>74</sup>

followed by acetyl at the 3'-OH afforded **81**. Treatment then of **81** with mCPBA under phase transfer conditions offered an efficient transformation to **82**. A deprotection/protection strategy and finally phosphorylation at the 3'-OH afforded **84**. Phosphoramidite **84** was used to synthesise <sup>4</sup>FU-modified RNA with comparable yields to that of their unmodified counterparts, indicating the stability of <sup>4</sup>FU during RNA synthesis protocols. NMR and biophysical analysis revealed the <sup>4</sup>FU in an RNA strand adopts the typical North-type sugar conformation, with no observable distortion of the RNA structure. <sup>4</sup>FU is capable of being recognised and processed in the same manner as unmodified uridine (by RNase H1 and RNase H2 for instance). The magnitude of the <sup>19</sup>F NMR chemical shift was shown to be sensitive to secondary structure (though not sequence context), and therefore can usefully be used to discriminate between changes in the RNA secondary structure. <sup>4</sup>-F-Modified RNA is advantageous over 2'-F-modified RNA for

monitoring RNA structural dynamics and enzyme-mediated processing as the 2'-OH group is retained as a key feature of biologically relevant RNA.<sup>74</sup>

Recently, 4'-fluoro-uridine **78** has been reported by Sourimant *et al.*,<sup>75</sup> to be a candidate broad spectrum antiviral for RNA viruses, showing activity against several strains of respiratory syncytial virus (RSV) and severe acute respiratory syndrome coronavirus 2 (SARS-CoV-2) alpha, gamma and delta variants.<sup>75</sup> In this study, 4'-Fluoro-uridine triphosphate **68** was assayed *in vitro* against RSV and SARS-CoV-2 RNA-dependent RNA polymerase (RdRP) and its mode of action was revealed to be *via* transcriptional stalling after incorporation into the growing oligomer. 4'-Fluoro-uridine **78** was also shown to possess high metabolic stability in human airway epithelial (HAE) cells and to be orally efficacious in animal models (5 mg kg<sup>-1</sup>, in RSV-infected mice and 20 mg kg<sup>-1</sup> in ferrets infected with different SARS-CoV-2 variants).<sup>75</sup>





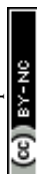
Scheme 8 Synthesis of 2'-OMe,4'-fluoro-uridine **89** and phosphoramidite derivative **91** as described by Malek-Adamian *et al.*<sup>76</sup>

2'-OMe,4'-Fluoro-uridine **89** was prepared Malek-Adamian *et al.*<sup>76</sup> in order to evaluate the effect of fluorine incorporation at the 4' position of uridine and to investigate the consequences on the subsequent thermal stability of DNA and RNA complexes. Fluorination of 2'-OMe,4',5'-dehydrouridine **85**, prepared from Appel iodination of 2'-OMe-rU followed by elimination with DBU, was accomplished by slow addition of  $I_2$  to a suspension of AgF and **85**. The resultant **86** was subjected to benzylation to afford **87**, which after treatment with mCPBA generated **88**, after migration of the benzoyl group to the 5'-OH position. Treatment of **88** with methanolic ammonia gave the unprotected 2'-OMe,4'-fluorouridine **89**, which was converted to its phosphoramidite derivative **91** (Scheme 8). The resultant **91** was incorporated into DNA and RNA oligonucleotides. As expected, computational studies on 2'-OMe,4'-fluoro-uridine suggested that it adopted a North sugar pucker, influenced by both electronic and steric effects. The 2'-OMe,4'-fluoro-uridine analogue modulated the binding affinity of parent 2'-modified homo and heteroduplexes and was found to destabilise DNA:DNA duplexes, although it had a slightly stabilising effect on DNA:RNA hybrids and RNA:RNA duplexes. These observations for DNA:RNA duplexes in particular allow a potential use in CRISPR/Cas9 technologies. The authors proposed application for siRNA and guide RNAs, allowing minimal disruption of structure and thermal stability upon incorporation, while allowing the introduction of this foreign nucleotide to serum nucleases and immunostimulatory receptors. The effect of the 2'-OMe,4'-fluoro-uridine analogue **89** on the gene silencing activity of siRNA duplexes has been explored.<sup>77</sup> siRNA modified with **89** was transfected into HeLa cells and was shown to silence both firefly luciferase and renal cell carcinoma (DRR) gene targets, especially when located at the 3'-overhang of the guide strand.<sup>77</sup> The authors hypothesised that enhanced nuclease stability along with a favourable interaction with the PAZ domain of human argonaute-2 protein improved the activity of the modified siRNA.

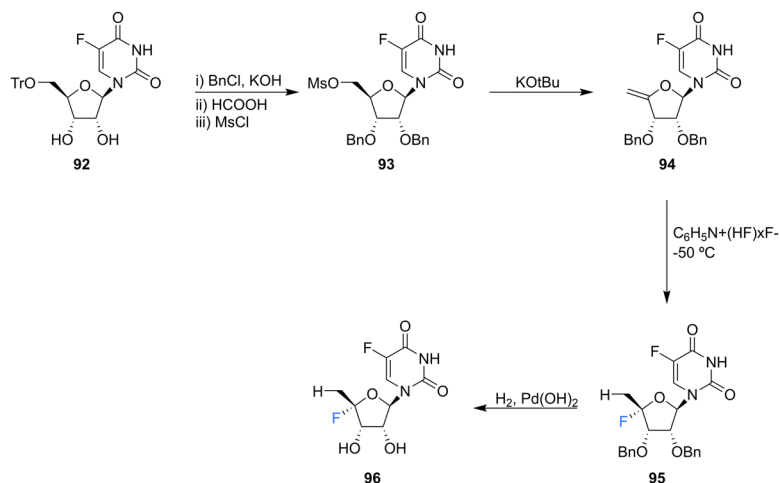
5'-Deoxyfluorouridine has been investigated as a prodrug to 5-fluorouracil, a cytotoxic chemotherapy medication used to

treat a variety of cancers.<sup>79–81</sup> The lack of a 5'-hydroxyl on 5'-deoxyfluorouridine prevents its intracellular conversion to nucleotides and its cytotoxicity is dependent on enzyme mediated (uridine phosphorylase) cleavage of its glycosidic bond. In an effort to improve on the design of this prodrug, Ajmera *et al.*, sought to obtain a derivative with a greater  $V_{max}$  for glycosidic bond cleavage by uridine phosphorylase, such that it would enhance the rate of accumulation of 5-fluorouracil in tumour tissues.<sup>78</sup> Ultimately a strategy utilising benzyl protection provided a suitable route to the targeted 5'-deoxy-4',5'-difluorouridine **96**, see Scheme 9. Briefly, **96** was prepared through benzylation and then trityl deprotection and mesylation at C5' of **92**. Treatment of mesylate **93** with potassium *tert*-butoxide afforded 4'-exo-olefin **94**, which was then hydrofluorinated with pyridinium poly(hydrogen fluoride) to generate **95** in very good yield, free from the  $\alpha$ -L-lyxo isomer. Hydrogenation of **95** with Pearlman's catalyst in anhydrous dioxane furnished 5'-deoxy-4',5'-difluorouridine **96**. In the event fluorouracil base release from uridine **96** was approximately 500 times more rapid than from the non-fluorinated analogue under acidic conditions, although it showed reasonable stability at neutral pH. The  $V_{max}$  for hydrolysis by uridine phosphorylase was 5-fold greater than that for 5'-deoxyfluorouridine, and a  $K_m$  10-fold lower, thus a  $V_{max}/K_m$  ratio 50-fold greater. Preliminary data revealed 5'-deoxy-4',5'-difluorouridine **96** was able to inhibit the growth of L1210 cells (mouse lymphocytic leukemia cell line), in line with the favourable uridine phosphorylase catalysed hydrolysis and release of the cytotoxic parent drug, 5-fluorouracil.<sup>78</sup>

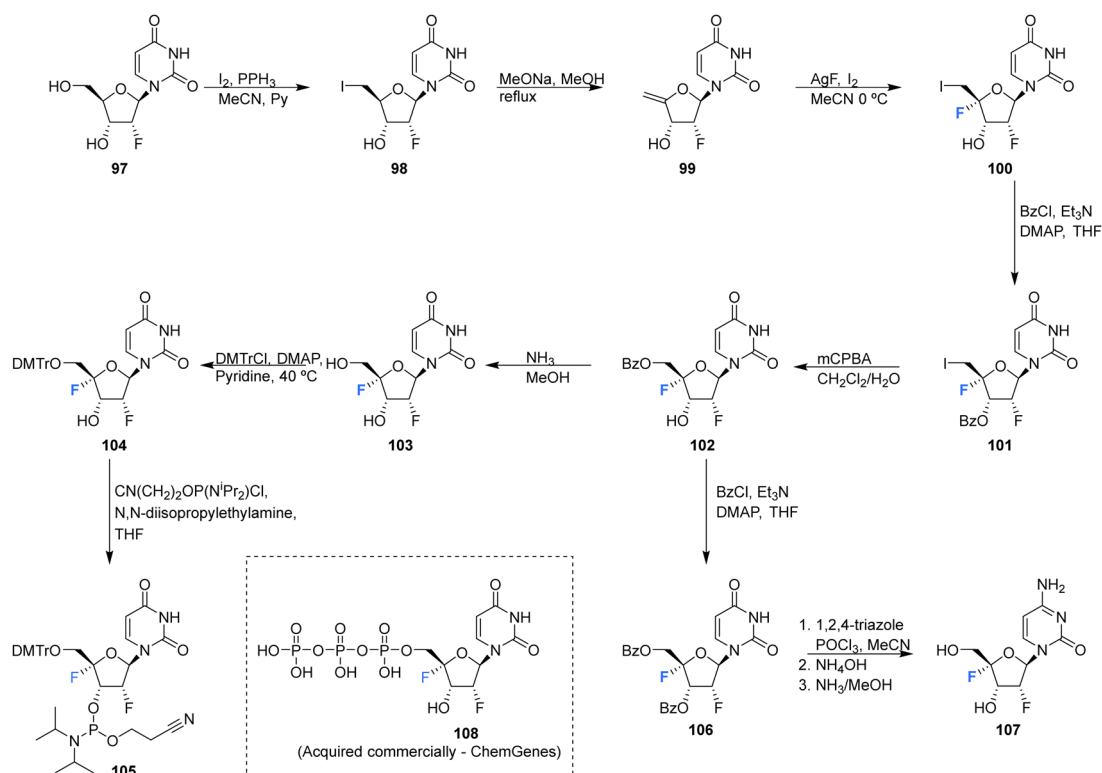
The syntheses of 2',4'-difluorinated nucleoside analogues, 2'-deoxy-2',4'-difluoro-uridine (2',4'-diF-rU) **103** and 2'-deoxy-2',4'-difluoro-cytidine (2',4'-diF-rC) **107** were accomplished by Martínez-Montero *et al.*, in 2014 using a common synthesis strategy.<sup>64</sup> 2'-Deoxy-2'-fluoro-uridine **97** was iodinated under Appel conditions and the resulting iodo-adenosine **98** was then susceptible to elimination in the presence of sodium methoxide, followed by iodofluorination after gradual addition of iodine/AgF. The route is illustrated in Scheme 10. The 5'-iodine was then







Scheme 9 Synthesis of 5'-deoxy-4',5-difluorouridine **96** as described by Ajmera *et al.*<sup>78</sup>



Scheme 10 Synthesis of 2'-deoxy-2',4'-difluorouridine (2',4'-diF-rU) **103**, 2',4'-deoxy-2',4'-difluorocytidine (2',4'-diF-rC) **107** and phosphoramidite **105** as described by Martínez-Montero *et al.*<sup>64,82</sup>

displaced with mCPBA to afford **102** after benzylation at the 3' position, a modification which appears to assist displacement through migration to the 5' position. Deprotection of **102** gave 2',4'-diF-rU **103**. The cytidine analogue 2',4'-diF-rC **107** was accessed after conversion of uracil **102** to a cytosine by benzoyl protection followed by installation of an amine at the 4 position of the base *via* a triazole intermediate and deprotection with ammonia. A combination of NMR and computational studies confirmed that installation of a 4'-fluorine onto 2'-fluoro-uridine provides a tool, driven by stereoelectronic effects, to promote a strong conformational "lock"

toward a pure North-type conformation.<sup>64</sup> Previous attempts to enforce such a "lock" had required a bicyclic framework linking the 2'- and 4'-positions at the ribofuranose sugar. 2',4'-DiF-rU **103** revealed a minimally destabilising character when studied in DNA:RNA duplexes, offering potential for gene editing technologies<sup>76</sup> The triphosphate of 2',4'-diF-rU, **108**, was acquired commercially by custom synthesis and evaluated as a substrate for HCV NS5B RNA polymerase. 2',4'-DiF-rUTP **108** was found to inhibit RNA synthesis primarily at the at the level of initiation in dinucleotide-primed reactions, with an IC<sub>50</sub> of 54.7 μM.



The phosphoramidite derivative of **103** was prepared by Martínez-Montero *et al.*, in 2015 following standard procedures as summarised in Scheme 10.<sup>82</sup> Protection of the 5'-hydroxyl of **103** using DMTr chloride generated **104**, which was then subjected to phosphitylation using CIP(OCeT)N(<sup>t</sup>Pr)<sub>2</sub> to furnish phosphoramidite **105**. Solid phase synthesis was then used to synthesise DNA and RNA oligonucleotides containing 2',4'-DiF-rU **103** units, with reported coupling yields of ~80% for phosphoramidite **105**. UV thermal duplex denaturing studies, along with molecular dynamics simulations, and NMR observations, revealed the North conformation adopted by 2',4'-DiF-rU **103** was maintained in DNA and RNA oligonucleotide duplex structures. The 2',4'-diF-RNA modification generated greater distortions in DNA:RNA duplexes when compared to 2'-F-RNA, and was not well tolerated in DNA:DNA duplexes. This modification was met with a relatively unique neutral response when incorporated into RNA:RNA duplexes, as it is capable of reinforcing the North sugar conformation without the increase thermal stability associated with the incorporation of locked bicyclic nucleoside analogues.<sup>82</sup> Such properties are particularly advantageous for siRNA-mediated gene silencing applications.<sup>83</sup>

2'-C-Modified-4'-fluoro-uridine analogues **135–137**, along with their phosphoramidate **141–146** and triphosphate derivatives **138–140**, were prepared by Wang *et al.*, to investigate their use as inhibitors of dengue virus (DENV) RNA-dependent RNA polymerase (RdRp).<sup>84</sup> Firstly, the 2'-C-modified uridines were synthesised from **109**, involving Dess-Martin oxidation and subsequent treatment with the appropriate Grignard reagent to acquire **111–113**, as shown in Scheme 11a. Conversion of the 2'-OH to its benzoate, followed by coupling with uracil, under Vorbrüggen glycosylation conditions and deprotection, furnished 2'-C-modified-uridines **117–119**. 2'-C-Modified-4'-fluoro-uridine analogues **135–137** were then acquired from **117–119**, using the general strategy of fluorinating 2'-C-modified-4',5'-olefins **123–125**, followed by oxidative hydrolysis and deprotection to afford **135–137**, as shown in Scheme 11a. Triphosphates **138–140** were synthesised using a single step strategy and the phosphoramidate prodrug analogues **141–146** were acquired using the phosphoryl agents as shown in Scheme 11b and c.

**135–137** and their analogues were assayed for their ability to both inhibit RNA replication by DENV RNA-dependent RNA polymerase (RdRp) and to be incorporated into a host mitochondrial DNA-dependent RNA polymerase (POLRMT), which potentially leads to mitochondrial dysfunction *in vivo*. 2'-C-Modified-4'-fluoro-uridine analogues **135–137** were found to be inactive against dengue virus in cell-based assays. 4'-Fluorination had an overall less deleterious effect on RdRp IC<sub>50</sub> than 2'-fluorination, whilst reducing POLRMT single nucleotide incorporation rate (SNIR). Triphosphate **139** exhibited an SNIR by POLRMT at background levels, whilst effecting a 2-fold improvement in DENV RdRp inhibition when compared to its non fluorinated derivative. Triphosphate **139** was also shown to be a poor substrate for mitochondrial DNA polymerase and the phosphoramidate prodrug **145** was revealed to be a promising candidate as it displayed potent anti-DENV cellular activity (EC<sub>50</sub> = 0.57 μM) whilst showing no cytotoxicity in any cell lines tested and it did not effect mitochondrial

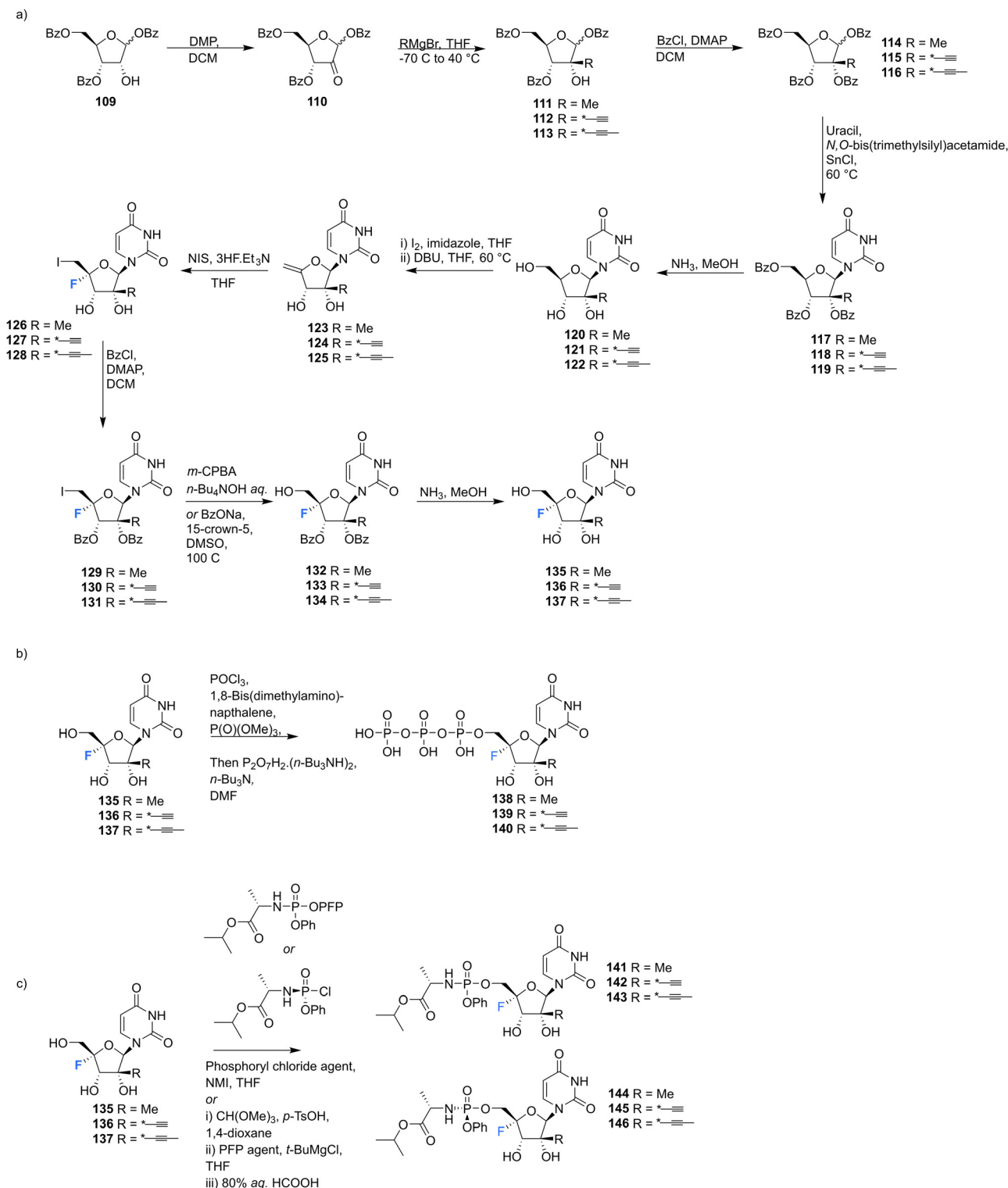
protein synthesis in prostate metastatic carcinoma cells (CC<sub>50</sub> > 200 μM). Thus this study revealed that 4'-fluorination of 2'-C-modified uridine analogues can lead to phosphoramidate prodrugs with significantly reduced SNIR by POLRMT and a maintained ability to inhibit DENV RdRp inhibition.<sup>84</sup>

2'-C-Substituted-4'-fluoro-uridine analogues **157**, **158**, **135**, **168**, **170** and **179–182** were synthesised and assayed for HCV NS5B inhibition, host polymerase inhibition, and HCV replicon activity.<sup>35</sup> To access **154**, the synthesis began with PMB protection of the uracil base of **147** and benzyl protection of the ribose hydroxyls to afford **149**. Oxidative cleavage and reduction of **149** afforded **150**, which was subjected to fluorination, *via* mesylation, with TBAF. Deprotection of **151** generated **152**, which was used to generate olefin **154** and this was progressed in a similar manner to analogues **155** and **156**, to generate the 4'-fluorinated analogues **157**, **158** and **135**, as summarised in Scheme 12.

3'-Ethynyl-5'-fluoro-uridine **161** was prepared from **158** by generating ketone **160** and subjecting this to a Grignard reaction, followed by subsequent desilylation. 2'-C-Substituted-4'-fluoro-uridine analogues **168** and **170**, were acquired from **162**. Cyclopentylidene protection of the 2' and 3' hydroxyls, followed by iodination at the 5' position afforded **164**. The established strategy of olefin generation then iodofluorination followed by hydroxydeiodination generated **165**, which was progressed to either **168** or **170** by controlled hydrogenation followed by hydrolysis. Uridine analogues **179–182** were then synthesised from **171–174** following established routes as summarised in Scheme 12.<sup>35</sup> Several uridines generated in this study were explored as their 5'-triphosphate derivatives in viral and human polymerase assays. Many of these were shown to be potent inhibitors of HCV NS5B polymerase (most notably the triphosphate of **135** and **181** with IC<sub>50</sub> values of 0.14 and 0.11 μM respectively), and showed little or no inhibition of human DNA and RNA polymerases. The 5'-triphosphate of **135** was used to investigate the mechanism of inhibition and was shown to be effective at terminating chain elongation by HCV NS5B polymerase. These results indicate that fluorination at the 4'-position does not alter the nucleosides inhibitory properties of NS5B dramatically and can lead to more potent NTPs targeting this polymerase. A range of 5'-phosphoramidate and 5'-bisphosphoramidate derivatives of uridines **157**, **158**, **135**, **168**, **170** and **179–182** were used in cell-based assays. From this study the 5'-phosphoramidate analogue of **135**, **183** (AL-335), was established as a lead compound, demonstrating high potency in HCV subgenomic replicon assays (EC<sub>50</sub> = 0.07 μM) and a promising cytotoxicity profile (CC<sub>50</sub> > 96 μM in six cell lines). In light of its excellent *in vitro* and *in vivo* properties, **183** was advanced to clinical development where it showed promising results in Phase 1 and 2 trials.<sup>35</sup>

The 4'-fluoro derivative of gemcitabine **184**, an antitumor drug with broad spectrum activity against RNA viruses, along with its phosphoramidate prodrug was recently synthesised by Zheng *et al.*, and assessed for its antiviral activity against the varicella zoster virus (VZV), the human cytomegalovirus (HCMV) and the severe acute respiratory syndrome coronavirus 2



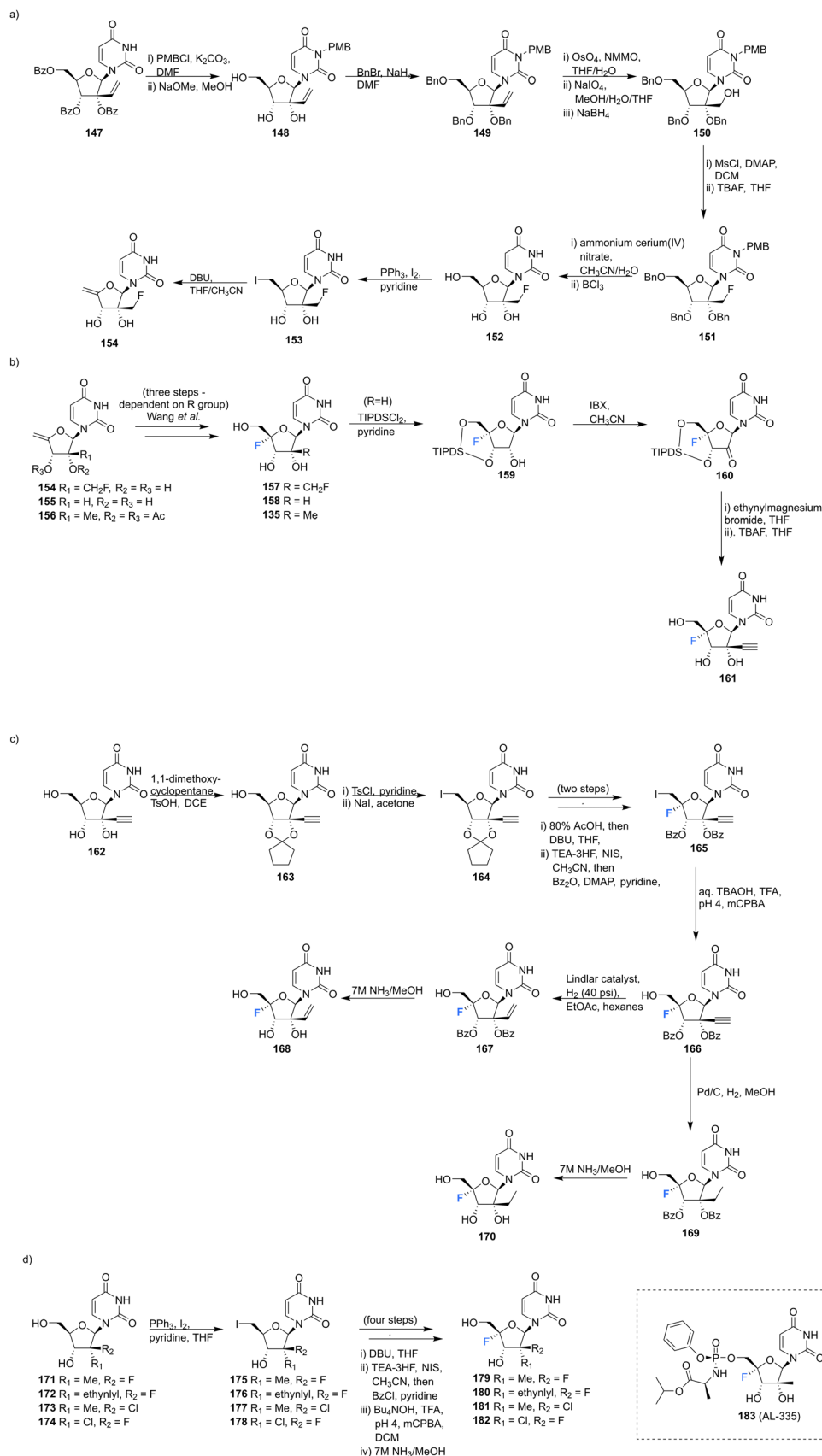


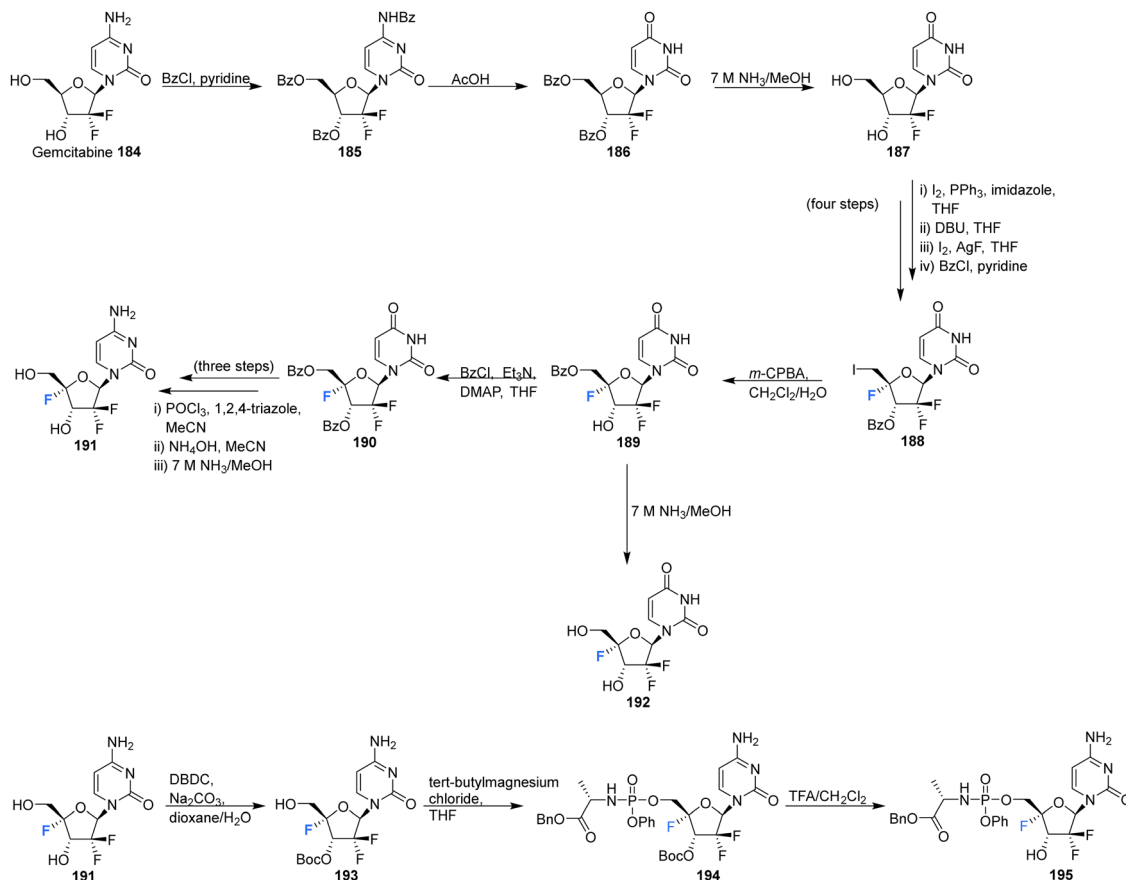
**Scheme 11** Synthesis of 2'-C-modified-4'-fluoro-uridine analogues **135–137**, triphosphates **138–140** and phosphoramidates **141–146** as described by Wang *et al.*<sup>84</sup>

(SARS-CoV-2).<sup>85</sup> The rationale being that modification at the 4'-position will increase its specificity as an antiviral agent by reducing its activity against host ribonucleotide reductases and polymerases.

4'-Fluoro-gemcitabine **191** was acquired from gemcitabine **184** in a route summarised in Scheme 13. It began with a three step sequence involving functional group protections, nucleobase deamination, and *O*-debenzoylation to obtain **187**. **187** was



Scheme 12 Synthesis of 2'-C-modified-4'-fluoro-uridine analogues **157**, **158**, **135**, **168**, **170**, **179–182** and **183** (AL-335) as described by Wang *et al.*<sup>35</sup>



Scheme 13 Synthesis of 4'-fluoro-gemcitabine **191**, 2'-difluoro-4'-fluoro-uridine **192** and phosphoramidate **195** as described by Zheng *et al.*<sup>85</sup>

then modified using established methods to install the 4'-fluoro motif using AgF and restore the 5'-O functionality with *m*-CPBA to generate protected 4'-fluoro-uridine **189**. Deprotection of **189** generated the 4'-fluoro-uridine analogue **192** whilst protection along with nucleobase conversion generated 4'-fluoro-gemcitabine **191**. The prodrug **195** of 4'-fluoro-gemcitabine was synthesised by selective protection at the 3'-position followed by treatment with phenyl aminoacyl phosphorochloridate and Boc deprotection, as illustrated in Scheme 13. 4'-Fluoro-gemcitabine **191** was observed to exhibit potent activity against VZV, HCMV, and SARS-CoV-2. Notably, when assayed against VZV the EC<sub>50</sub> was 0.042 μM, although it displayed significant cytotoxicity (CC<sub>50</sub> = 0.11 μM). The prodrug **195** showed reduced anti-VZV activity, though with an improved selectivity index (SI = 36). A similar, although slightly reduced, effect was observed against HCMV. When assayed against SARS-CoV-2 it displayed comparable antiviral activity (EC<sub>50</sub> = 0.73 μM) to its cytotoxic concentration in measurements of cell growth.<sup>85</sup>

#### 5.4 4'-Fluoro-deoxythymidines

Zhou *et al.* prepared 4'-fluoro-deoxythymidine **200** and the phosphoramidite **201**, as illustrated in Scheme 14,<sup>65</sup> using a similar strategy to that for the synthesis of 4'-fluoro-uridine **78** and its phosphoramidite derivative **84**. 4'-Fluoro-deoxythymidine **200** was found to adopt a North-type ribose ring pucker, which

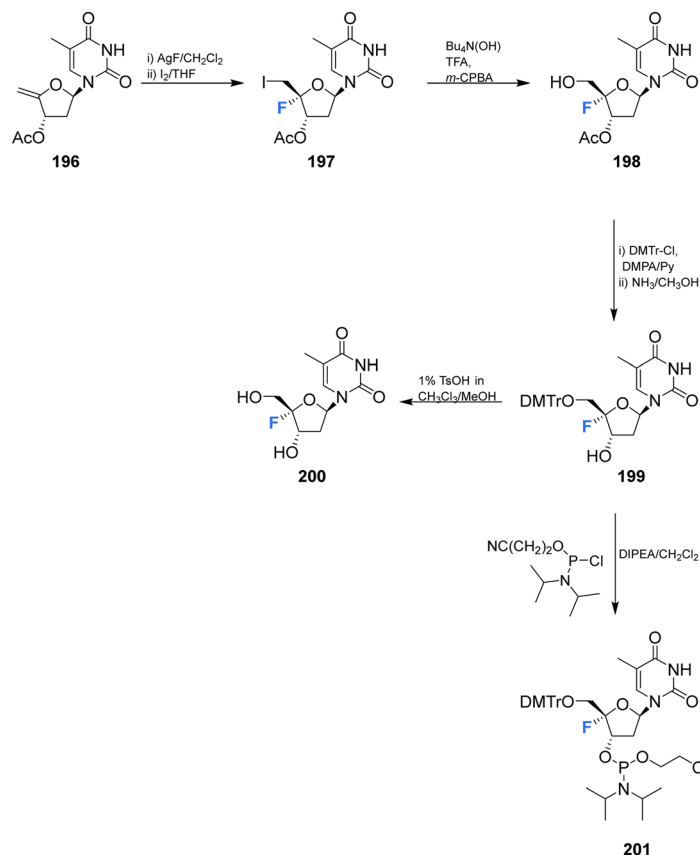
persisted when introduced to oligodeoxyribonucleotides (ODNs). This conformational tendency was maintained in ODN/cDNA and ODN/cRNA duplexes. The half-life for decomposition for 4'-fluoro-deoxythymidine **200** in pure water was recorded as 4 h, shorter than 4'-fluoro-uridine **81** (*t*<sub>1/2</sub> = 9 h). 4'-Fluoro-deoxythymidine **200** modified ODNs were found to be stable in neutral buffers, although the glycosidic bond of **200** was prone to scission under alkaline conditions. Through techniques such as circular dichroism spectroscopy, thermal denaturing and RNase H1 footprinting studies, 4'-fluoro-deoxythymidine **200** has been shown to resemble 2'-fluoro-deoxyribonucleotides but it imparts less structural perturbation to ODN/cDNA and ODN/cRNA duplexes, thus 4'-fluoro-deoxythymidine **200** represents a good <sup>19</sup>F-NMR probe for investigating RNA secondary structure and function.<sup>65</sup>

#### 5.5 2'-Deoxy-2',4'-difluoro-arabinouridines

2'-Deoxy-2',4'-difluoro-arabinouridine (2',4'-diF-araU) **208** was synthesised in a similar manner to that of **103** and **200**, but commencing with 2'-deoxy-2'-fluoro-arabinouridine **202**, an epimer of **97**, as shown in Scheme 15.<sup>86</sup> Incorporation into oligonucleotide duplexes required activation to phosphoramidite **210**. Briefly, **208** was treated with DMTr chloride to generate **209** and then subsequent phosphitylation with ClP(OCeN)(<sup>i</sup>Pr)<sub>2</sub> afforded **210** enabling its use in solid-phase oligonucleotide synthesis. 2',4'-DiF-araU **210** was found to be well tolerated in







Scheme 14 Synthesis of 4'-fluoro-deoxythymidine **200** and phosphoramidite derivative **201** as described by Zhou *et al.*<sup>65</sup>

DNA:RNA hybrid oligonucleotides, providing some improvement in thermal stability. The effect of the North-type pucker adopted by 2',4'-diF-araU **210** was observed in RNase H recruitment studies, where cleavage sites differed from the unmodified duplexes and degradation rates for the RNA strand were lower. Such results are thought to be promising for gene silencing applications.<sup>86</sup>

### 5.6 3',4'-Difluoro-3'-deoxyribonucleosides.

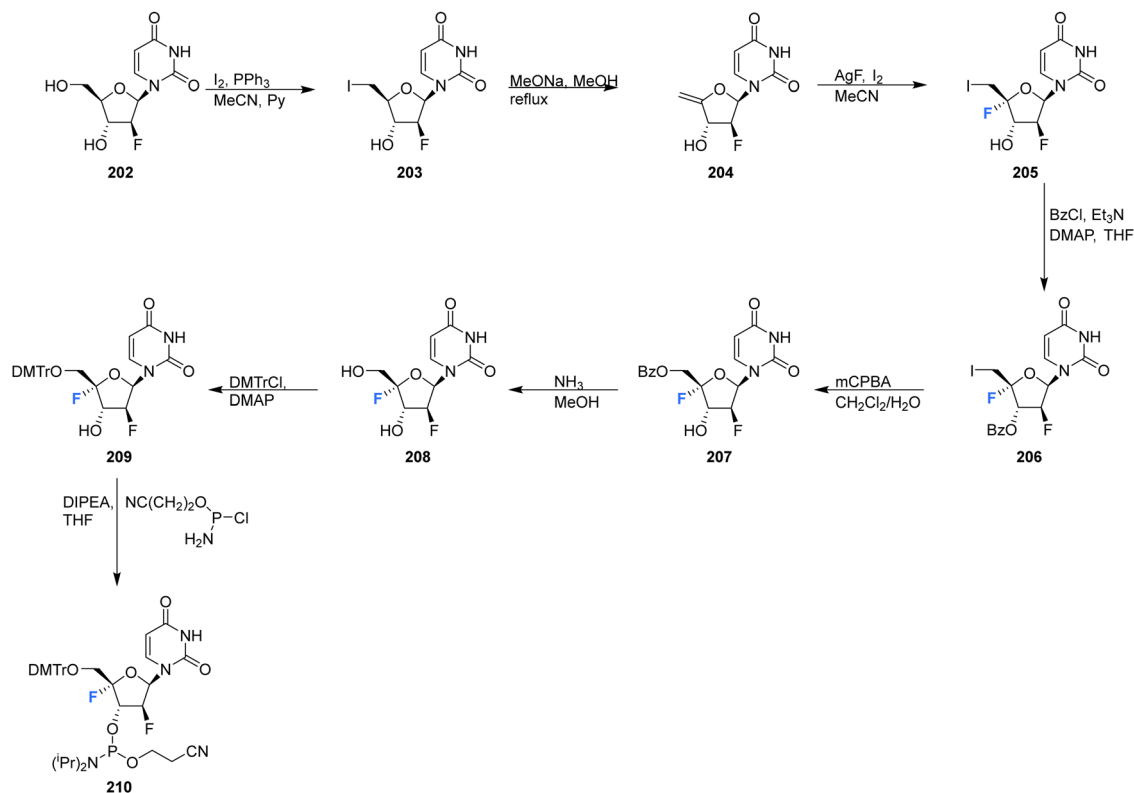
Shimada *et al.*, prepared several 3',4'-difluoro-3'-deoxyribonucleosides using a strategy involving di-fluorination of 3',4'-dehydro cytosine and adenine nucleosides with  $\text{XeF}_2/\text{BF}_3 \cdot \text{OEt}_2$ .<sup>66</sup> Briefly, for **215**, **216** and **219**, protected nucleosides **212** and **217** were first acquired through de-acylation and silylation of **211**, and then treated with  $\text{XeF}_2$  and  $\text{BF}_3 \cdot \text{OEt}_2$  in  $\text{Et}_2\text{O}$  at  $0^\circ\text{C}$ . In order to separate the stereoisomers produced, the silyl-protecting groups were exchanged for acetates, and this allowed for isolation of  $\alpha/\beta$ -anti/*syn* adducts as illustrated in Scheme 16. The  $\alpha/\beta$  preference in these di-fluorination reactions was rationalised by the shielding of the  $\alpha$  face by the sterically demanding protecting groups. Finally, deprotection of **213**, **214** and **218** using  $\text{NaOMe}$  in  $\text{MeOH}$  furnished 3',4'-difluoro-3'-deoxyribonucleosides **215**, **216** and **219**. Access to the difluorinated adenine nucleosides **223**, **224**, **228** and **229** was achieved in a similar manner by di-fluorination of **220** and **225**, which, after  $N^6$ -pivaloylation, de-acylation and silylation allowed the isolation of stereoisomers **221**, **222**, **226** and **227**. Deprotection then

provided the di-fluorinated adenosines **223**, **224**, **228** and **229**. The stereochemical outcome of the adenine derivatives was largely consistent with that observed for the 3',4'-difluoro-3'-deoxycytidines, although the authors noted that the  $\alpha$ -*syn*-adduct selectivity was unexpected after fluorination of **225**, suggesting a role for the sterically demanding adenine base. 3',4'-Difluoro-3'-deoxyadenosines **223**, **224**, **228** and **229** were assayed for activity against murine leukemia cells and human cervix carcinoma, although none showed any inhibitory activities. Additionally, no antiviral activity was observed for **223**, **224**, **228** and **229** against human cytomegalovirus, herpes simplex virus, vesicular stomatitis virus and varicella-zoster-virus, though no cytotoxicity against the host cells (at  $100 \mu\text{M}$ ) was observed either. Promisingly, 3',4'-difluoro-3'-deoxyadenosine **228** exhibited inhibitory activity in anti-HCV assays ( $\text{EC}_{50} = 4.7 \mu\text{M}$ ). Interestingly the parent candidate, cordycepin, a non-fluorinated analogue which has shown antitumour activity, exhibited no such significant anti-HCV activity, whilst 3'-fluoro-cordycepin exhibits anti-HCV activity ( $\text{EC}_{50} = 1.2 \mu\text{M}$ ) but is highly toxic to host cells. Thus the incorporation of fluorine to the 4'-position of 3'-fluoro-cordycepin can be rationalised to have decreased its cytotoxicity, whilst retaining its inhibitory activity against HCV.

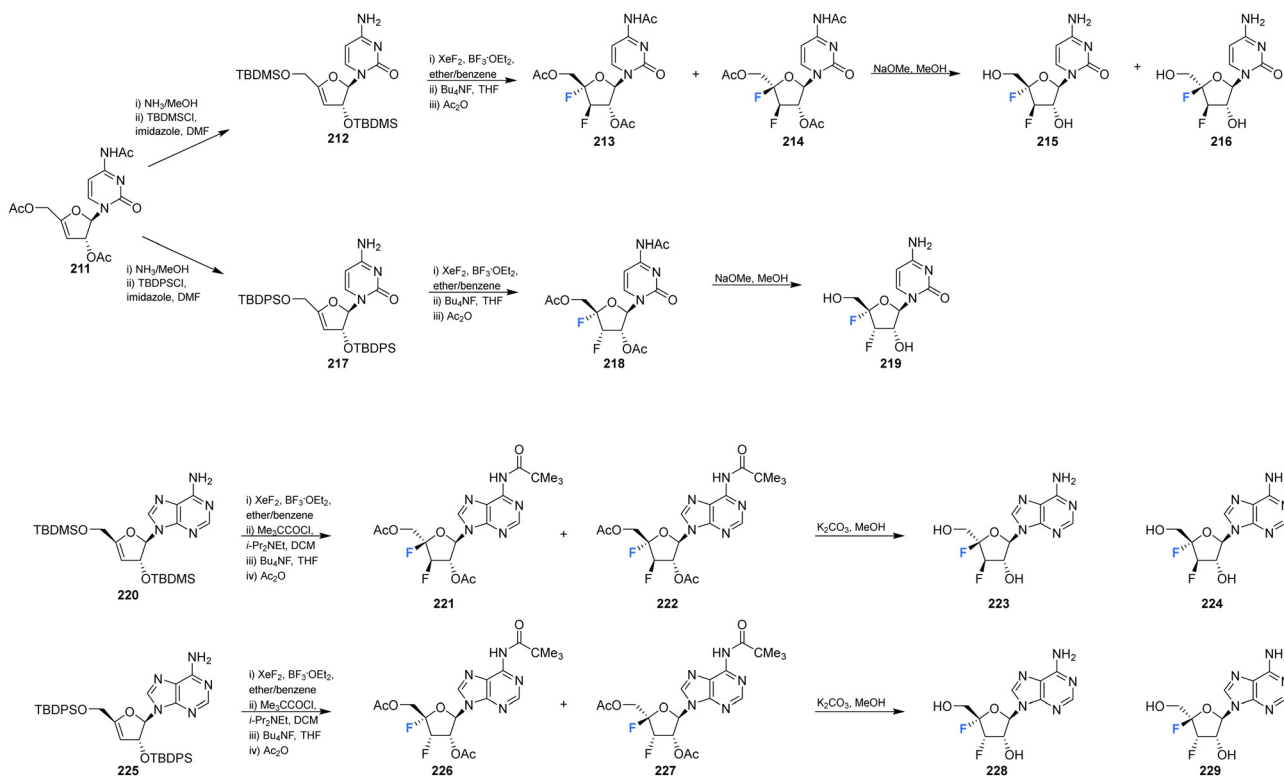
### 5.7 4'-Fluoro-guanosines

4'-Fluoro-guanosine prodrugs **235**, **236** and **238**, reported in the patent literature by Mayes *et al.*,<sup>69</sup> were synthesised using a



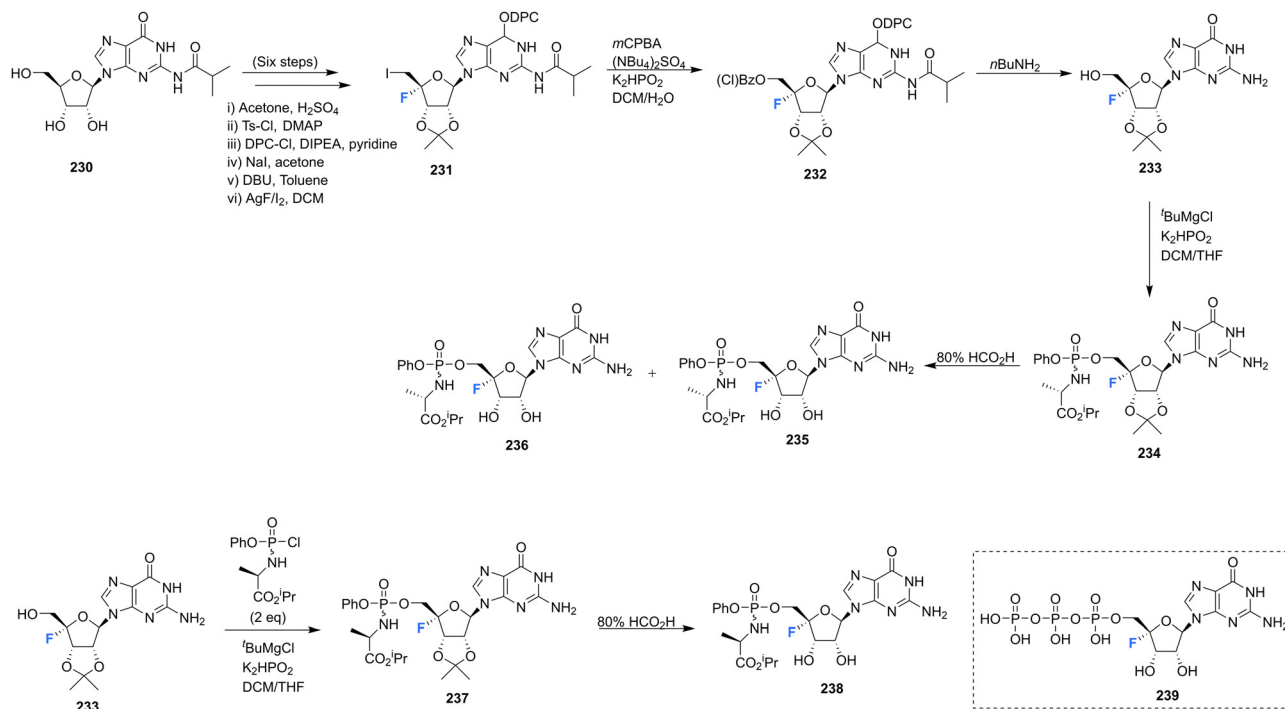


**Scheme 15** Synthesis of 2'-deoxy-2',4'-difluoro-arabinouridine (2',4'-diF-araU) **208** and phosphoramidite derivative **210** as described by Martinez-Montero *et al.*<sup>86</sup>



**Scheme 16** Synthesis of 3',4'-difluoro-3'-deoxycytidines **215**, **216** and **219** and 3',4'-difluoro-3'-deoxyadenosines **223**, **224**, **228** and **229** as described by Shimada *et al.*<sup>66</sup>





Scheme 17 Synthesis of 4'-fluoro-guanosine prodrugs **235**, **236**, **238** and 5'-O-triphosphate **239** synthesised by Mayes *et al.*<sup>69</sup>

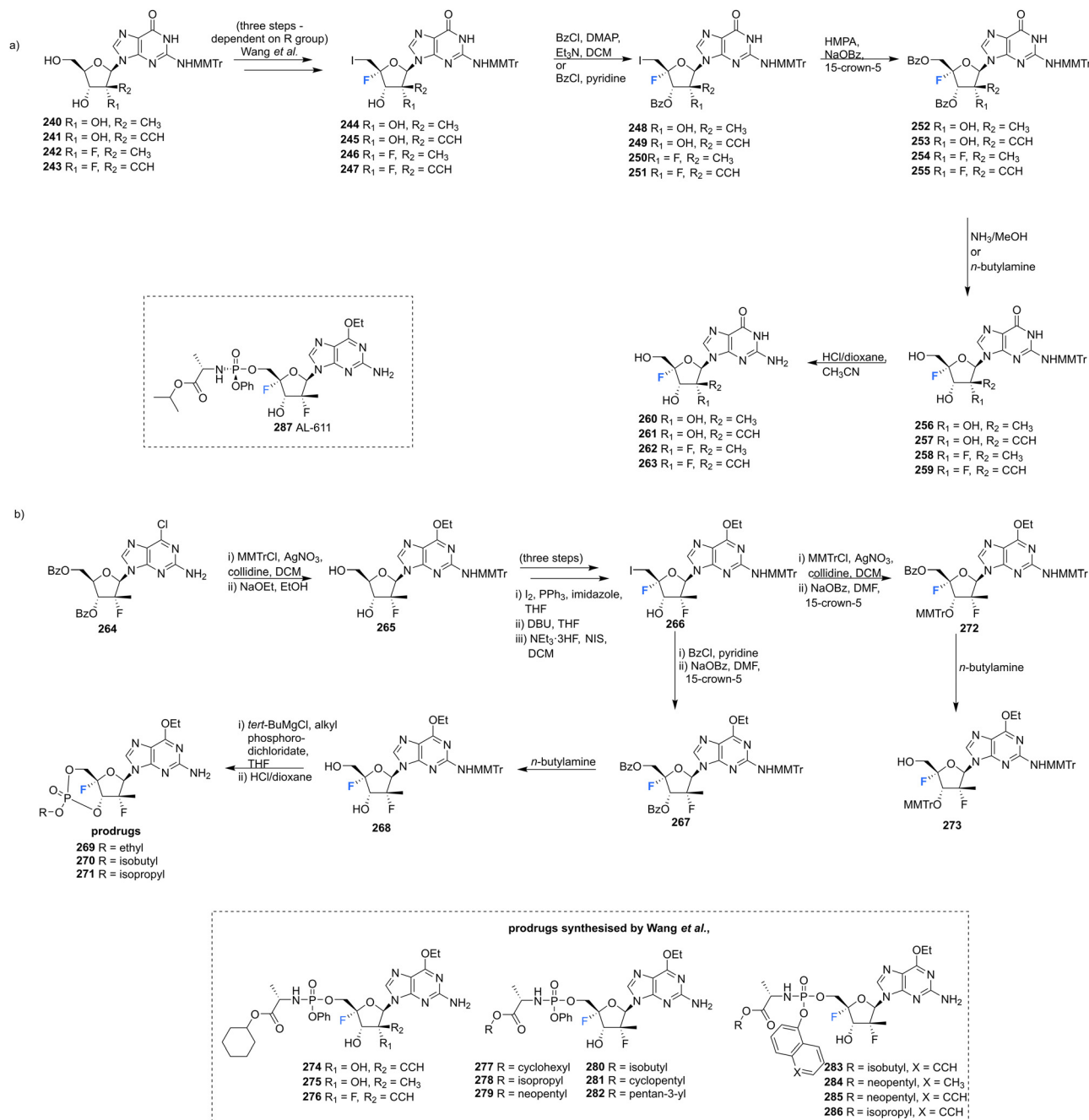
strategy outlined in Scheme 17. Protected guanosine **231** was generated from **230** in six steps using established methods. Reaction of **231** with *m*CPBA followed by *n*-butyl amine generated **233**, which was then coupled with the appropriate chlorophosphoramidate to afford **235**, **236** and **238**, after deprotection. These compounds were then purified by semi prep HPLC. Prodrugs **235**, **236** and **238** were assayed for HCV replicon activity and cytotoxicity. Diastereoisomers **235** and **236** both demonstrated  $\text{CC}_{50}$  values with the range of 1–10  $\mu\text{M}$ , though differed substantially with regards to  $\text{EC}_{50}$  with **235** having a value  $>10 \mu\text{M}$  and **236** between 250 nM–1  $\mu\text{M}$ . Single isomer **238** demonstrated a  $\text{CC}_{50}$  value within the range of 1–10  $\mu\text{M}$  and a  $\text{EC}_{50} > 10 \mu\text{M}$ . The pharmacokinetics of these prodrugs were also studied for each compound measured by LC-MS/MS in mouse liver samples. **235** and **238** were found to accumulate in these studies, significantly less so when compared to **73** and **74** (uracil analogues reported in the same study, Scheme 6), and **236** was not detected at all. The triphosphate **239** was also synthesised and was assayed for inhibitory activity against purified HCV polymerase, demonstrating an  $\text{IC}_{50} \leq 250 \text{ nM}$ .<sup>69</sup>

A series of 2'-C-substituted-4'-fluoro-guanosine analogues were also prepared by Wang *et al.*, and assayed for HCV NS5B inhibition, host polymerase inhibition, and HCV replicon activity (Scheme 18).<sup>87</sup> **260**–**263** were prepared using already established procedures from  $N^2$ -monomethoxytritylated guanosines **240**–**243**. The 5'-O-triphosphate derivatives of each 2'-C-substituted-4'-fluoro-guanosine were also synthesised and assayed against HCV NS5B and human polymerases. Each 2'-C-substituted-4'-fluoro-guanosine **260**–**263** was a potent inhibitor of the HCV NS5B polymerase, with the triphosphate of **261** revealing

an increased potency ( $\text{IC}_{50} = 0.14 \mu\text{M}$ ) when compared to its non-fluorinated analogue ( $\text{IC}_{50} = 0.42 \mu\text{M}$ ) and the triphosphate of **263** ( $\text{IC}_{50} = 0.16 \mu\text{M}$ ) a comparable potency relative to its non-fluorinated analogue ( $\text{IC}_{50} = 0.099 \mu\text{M}$ ). Chain termination assays indicated that the triphosphate of **263** induced immediate chain termination. Triphosphates of **260**–**262** did not demonstrate any inhibition of human DNA polymerases  $\alpha$ ,  $\beta$ , and  $\gamma$  and RNA polymerase II. The triphosphate of **263** showed low level inhibition of human DNA pol- $\alpha$  and no inhibition of human DNA polymerases  $\beta$ ,  $\gamma$  and RNA polymerase II.<sup>87</sup>

In order to effectively test in cell-based assays, and to circumvent poor *in vivo*, monophosphorylation, nucleosides **269**–**271** and **274**–**286** were synthesised as 6-OEt monophosphate prodrugs. Monomethoxytritylation of the amino group of **264**, followed by fluorine installation at the 4'-position provided **266**. **266** was then progressed by nucleophilic substitution of the iodine, followed by protecting group protections/deprotections to furnish **268** and **273**. **268** was used to acquire cyclic phosphates **269**–**271** using the appropriate phosphodichloridate, and **273** was used to prepare the phosphoramidate prodrugs **277**–**286**. 5'-Phosphoramidate prodrugs of 2'-C-substituted-4'-fluoro-guanosine analogues **274**–**276** were acquired *via* their 3'-O, $N^2$ -bismonomethoxytrityl- $O^6$ -ethyl analogues using standard methods. Most prodrugs in this study demonstrated potent HCV subgenomic replicon activity and the 2',4'-difluoro-2'-C-methyl scaffold was prioritised for prodrug development, given the promising *in vitro* data of the precursor **262**. Ultimately from this scaffold the Sp-diastereoisomer **287** (AL-611,  $\text{EC}_{50} = 0.005 \mu\text{M}$ ,  $\text{CC}_{50} > 100 \mu\text{M}$  for both) was selected as a lead candidate for preclinical toxicology studies (Table 1).<sup>87</sup>





Scheme 18 Synthesis of 2'-C-modified-4'-fluoro-guanosine analogues **260–263**, cyclic phosphates **269–271** and phosphoramidates **274–286** as described by Wang *et al.*<sup>87</sup>

### 5.8 Non-canonical 4'-fluoro-ribonucleosides

This review has focused principally on canonical nucleosides modified at the 4'-position of the ribose with a fluorine atom, however it is important to note that there are examples in both the published and patent literature of 4'-fluoro-nucleosides containing non-canonical bases. For instance Wang *et al.*, prepared the 4'-fluoro-pyrimidine C-nucleoside analogue **300**, an of antiviral favipiravir, in 2016.<sup>88</sup> The coupling of ribolactone **291** with pyridine **292** generated hemiacetal **293**, the subsequent reduction and deprotection of which gave the desired β-epimer

**294**. The nitrile was then partially hydrolysed to amide **295**, followed by desilylation to afford C-nucleoside **296**. The introduction of the 4'-fluorine was accomplished after dehydration to enol ether **297** and then iodofluorination following a standard approach. Hydroxide displacement of **298** followed by aminolysis furnished 4'-fluoro-pyrimidine C-nucleoside **300**, see Scheme 19.<sup>88</sup> A neuraminidase activity-based assay using Darby canine kidney (MDCK) epithelial cells infected with influenza strain A/WSN/33 (H1N1) revealed **300** to possess only weak anti-influenza activity (EC<sub>50</sub> = 98 μM), CC<sub>50</sub> = 185 μM.



**Table 1** 4'-Fluoro-ribonucleosides with most notable biological activity and applications covered within this review

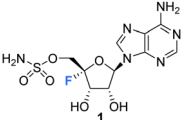
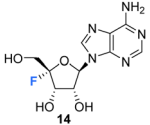
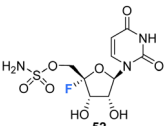
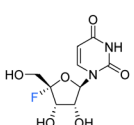
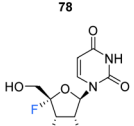
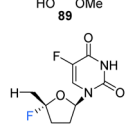
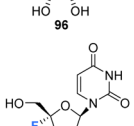
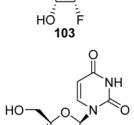
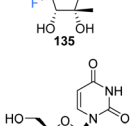
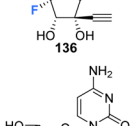
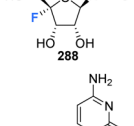
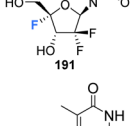
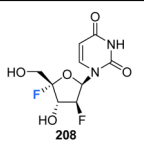
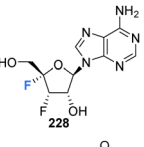
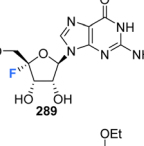
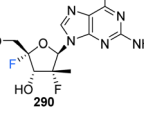
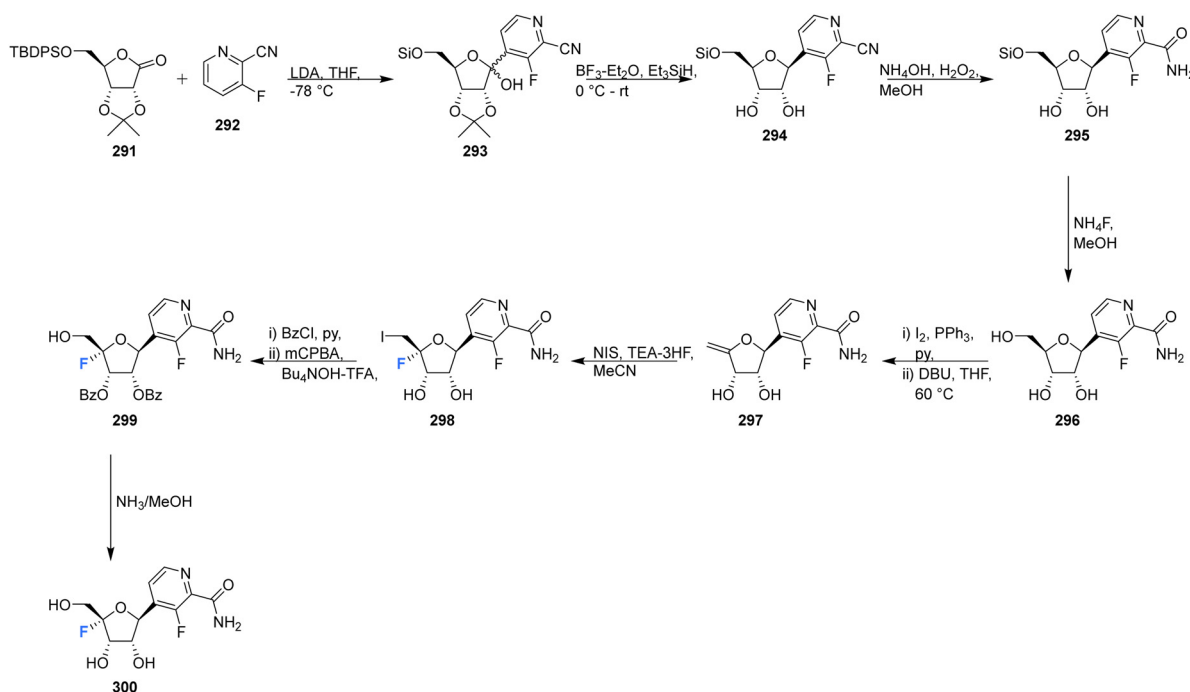
Compound (core scaffold)	Biological activity/application	Ref.
 <b>1</b>	Antibiotic <i>via</i> inhibition of protein synthesis. Highly toxic to mammals. Significant anti-trypanosomal and leishmanicidal activity.	38 and 43–50
 <b>14</b>	Inhibitor of <i>S</i> -adenosyl-L-homocysteine hydrolase activity ( $K_{\text{inact}} = 0.24 \text{ min}^{-1}$ and $K_i = 166 \text{ }\mu\text{M}$ ). Prodrug <b>43</b> – agonist for protein kinase 1 (ALPK1). Triphosphate <b>35</b> – inhibitor of HCV NTP-dependent RNA polymerase (NS5B, $\text{IC}_{50} > 10 \text{ }\mu\text{M}$ )	68, 69 and 72
 <b>52</b>	Exhibited considerably reduced antibacterial and cytotoxic properties when compared nucleocidin <b>1</b> .	73
 <b>78</b>	Broad spectrum antiviral for RNA viruses (RSV and SARS-CoV-2) Prodrugs <b>73</b> and <b>74</b> – HCV replicon activity, <b>73</b> ( $\text{EC}_{50} > 10 \text{ }\mu\text{M}$ ) and <b>74</b> ( $\text{EC}_{50}$ between 1–10 $\mu\text{M}$ ) and cytotoxicity ( $\text{CC}_{50}$ values within the range of 1–10 $\mu\text{M}$ ). Triphosphate <b>68</b> – inhibitor of HCV NTP-dependent RNA polymerase (NS5B, $\text{IC}_{50} = 2 \text{ }\mu\text{M}$ ). Phosphoramidite <b>84</b> – used as a $^{19}\text{F}$ NMR probe to impart conformational lock and to investigate RNA structure.	69, 71, 74 and 75
 <b>89</b>	Phosphoramidite <b>91</b> – used as a $^{19}\text{F}$ NMR probe to investigate DNA and RNA complexes. Gene silencing activity of siRNA duplexes modified with <b>89</b> .	76
 <b>96</b>	Inhibits growth of L1210 cells (mouse lymphocytic leukemia cell line), upon realisation of cytotoxic parent drug, 5-fluorouracil.	78
 <b>103</b>	Triphosphate <b>108</b> – inhibitor of HCV NTP-dependent RNA polymerase (NS5B, $\text{IC}_{50} = 54.7 \text{ }\mu\text{M}$ ). Phosphoramidite <b>105</b> – used as a $^{19}\text{F}$ NMR probe to impart conformational lock and to investigate DNA and RNA complexes.	64 and 82
 <b>135</b>	Prodrug <b>185</b> (AL-335) – demonstrated high potency and selectivity in HCV subgenomic replicon assays ( $\text{EC}_{50} = 0.07 \text{ }\mu\text{M}$ , $\text{CC}_{50} > 96 \text{ }\mu\text{M}$ ).	35
 <b>136</b>	Prodrug <b>145</b> – displayed anti-DENV cellular activity ( $\text{EC}_{50} = 0.57 \text{ }\mu\text{M}$ ) and no cytotoxicity.	84
 <b>288</b>	Triphosphate <b>71</b> – inhibitor of HCV NTP-dependent RNA polymerase (NS5B, $\text{IC}_{50}$ between 250 nM–1 $\mu\text{M}$ ).	69
 <b>191</b>	Inhibitory activity against VZV, HCMV, and SARS-CoV-2. Though significant cytotoxicity ( $\text{CC}_{50} = 0.11 \text{ }\mu\text{M}$ ). Prodrug <b>195</b> – inhibitory activity against VZV, HCMV, and SARS-CoV-2 with improved SI (36).	85
 <b>200</b>	Phosphoramidite <b>201</b> – $^{19}\text{F}$ -NMR probe for investigating RNA secondary structure and function.	65





Table 1 (continued)

Compound (core scaffold)	Biological activity/application	Ref.
	Phosphoramidite <b>210</b> – $^{19}\text{F}$ NMR probe to impart conformational lock and stability to investigate DNA and RNA complexes for applications in gene silencing.	86
	Inhibitory activity in anti-HCV assays ( $\text{EC}_{50} = 4.7 \mu\text{M}$ ), with no cytotoxicity against the host cells.	66
	Triphosphate <b>239</b> – inhibitor of HCV polymerase ( $\text{IC}_{50} \leq 250 \text{ nM}$ ) Prodrugs <b>235</b> , <b>236</b> and <b>238</b> – inhibitor of HCV replicon, <b>235</b> ( $\text{EC}_{50} > 10 \mu\text{M}$ , $\text{CC}_{50}$ between 1–10 $\mu\text{M}$ ) and <b>236</b> ( $\text{EC}_{50}$ between 250 nM–1 $\mu\text{M}$ , $\text{CC}_{50}$ between 1–10 $\mu\text{M}$ ). <b>235</b> ( $\text{EC}_{50} > 10 \mu\text{M}$ , $\text{CC}_{50}$ between 1–10 $\mu\text{M}$ ).	69
	Prodrug <b>287</b> ( <b>AL-611</b> ) – potent HCV subgenomic replicon activity ( $\text{EC}_{50} = 0.005 \mu\text{M}$ , $\text{CC}_{50} > 100 \mu\text{M}$ ).	87

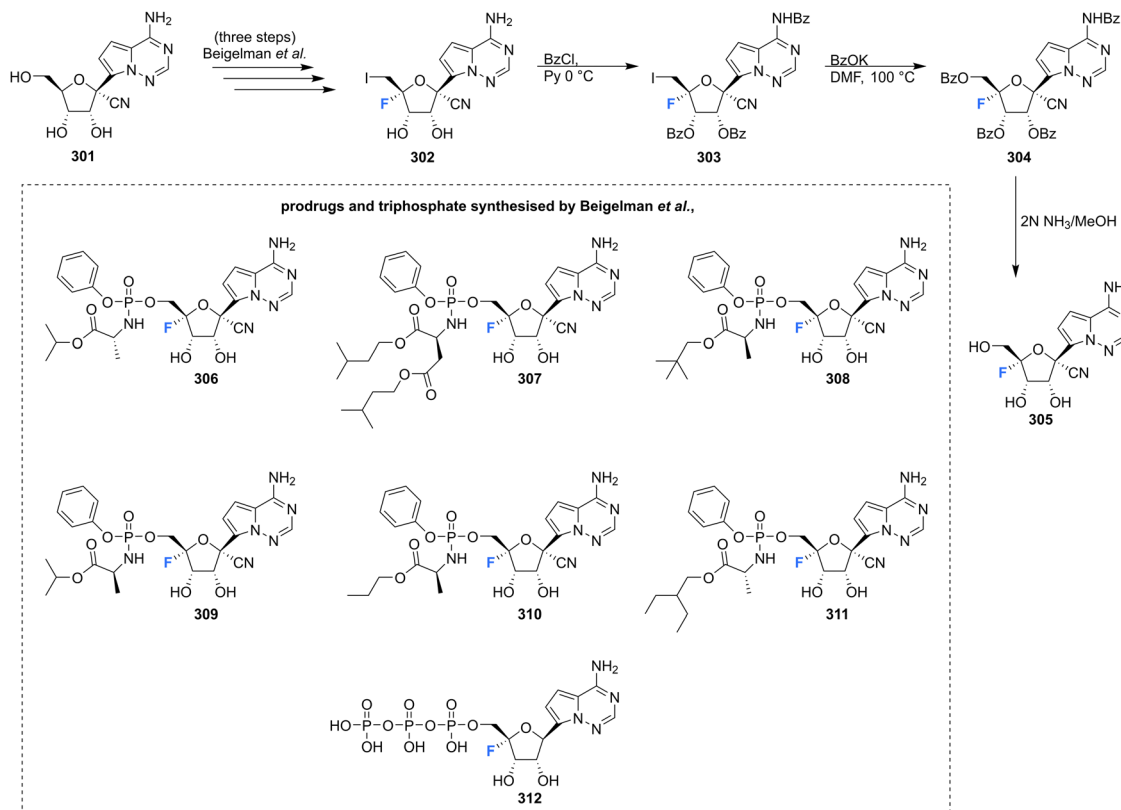
Scheme 19 Synthesis of 4'-fluoro-pyrimidine C-nucleoside **300** as described by Wang *et al.*<sup>88</sup>

*In vivo* nucleoside 5'-triphosphate (NTP) levels, a critical factor for *in vivo* efficacy, were assessed in A549 cells treated with **300**, and revealed very low to undetectable amount of NTPs.

4'-Fluoro-pyrrolo triazine adenosine analogue **305**, along with its triphosphate **312** and various prodrugs **306–311**, as shown in Scheme 20, have been reported in the patent literature.<sup>89</sup> Installation of 4'-fluorine in the 1'-cyano adenosine analogue **301** was accomplished using the established protocol, from which the

prodrugs **306–311** and triphosphate **312** were acquired using the appropriate phosphoryl agents. Prodrugs **306–311** displayed inhibitory activity against numerous viruses (EBOV, HRV 1B, OC43CoV, DENV, RSV), in many cases displaying  $\text{IC}_{50}$ 's  $\leq 1 \mu\text{M}$ , whilst presenting with  $\text{CC}_{50}$ 's  $> 100 \mu\text{M}$ . Triphosphate **312** was assayed against a polymerases derived from HRV16, HCV, DENV and RSV and displayed inhibition in all cases, with  $\text{IC}_{50}$ 's of 0.13, 0.4, 1.1, 0.03  $\mu\text{M}$  respectively.<sup>89</sup> These examples serve to highlight the





Scheme 20 Synthesis of 4'-fluoro-pyrimidine C-nucleoside **305** and prodrugs **306–311** and triphosphate **312** as described by Beigelman *et al.*<sup>89</sup>

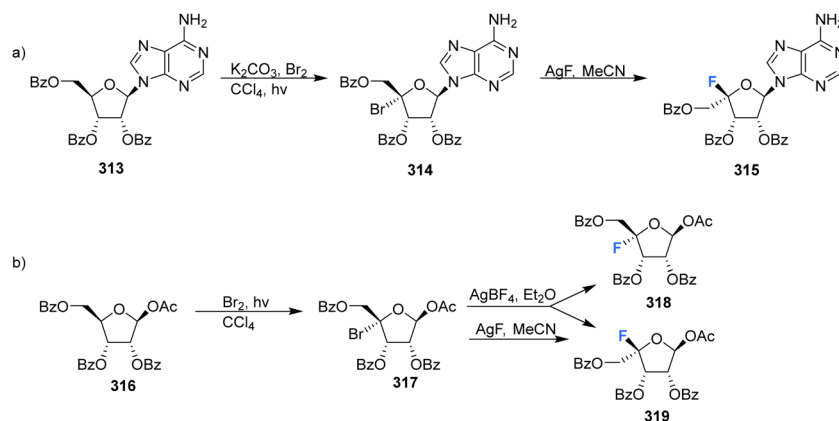
broadening attention afforded to the 4'-fluorination of nucleosides and demonstrate the potential that the 4'-fluoro-ribose motif has in the exploration of biologically active nucleosides.

## 6. Additional strategies for the preparation of 4'-fluorinated nucleosides

Many of the synthetic approaches outlined so far have relied on the fluorination of a protected 4',5'-dehydro-nucleoside using an appropriate fluorinating pseudohalogen. Whilst this has

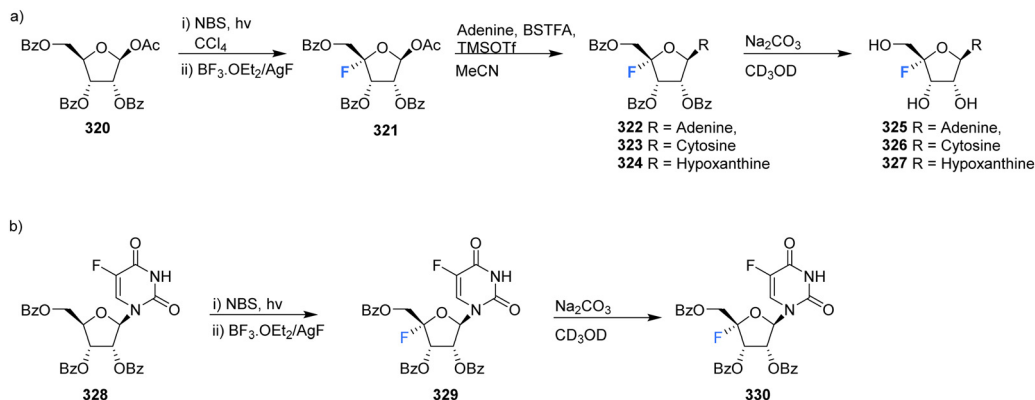
proven to be a relatively successful and widely used approach, other approaches have been developed over the years to access the 4'-fluororibose moiety.

Ferrier *et al.*, reported a strategy involving the photobromination of protected  $\beta$ -D-ribose, followed by fluorination of the subsequent 4'-bromoribose product, see Scheme 21.<sup>90</sup> Photobromination at the 4' position of adenosine **313** gave the unstable 4'-bromo-derivative **314**, which was isolated from a complex mixture but in low yield. The lyxo-fluoride **315** was subsequently generated from **314** upon treatment with silver fluoride although the conversions were also modest. In a similar manner, treatment

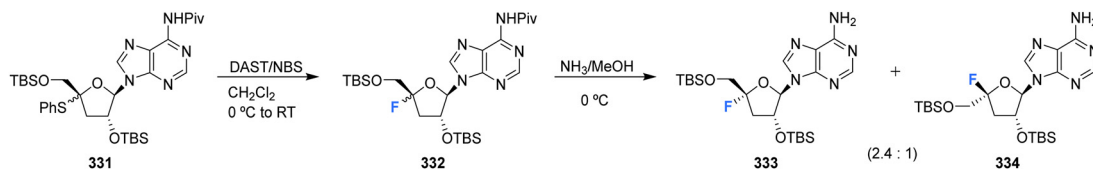


Scheme 21 Synthesis of 4'-fluoro-nucleosides by a bromination-fluorination protocol developed by Ferrier *et al.*<sup>90</sup>

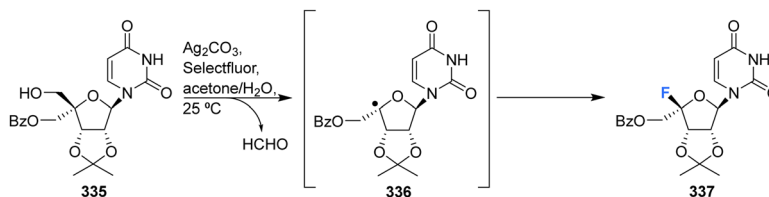




Scheme 22 Synthesis of 4'-fluoro-nucleosides by a bromination-fluorination protocol developed by Lee *et al.*<sup>70</sup>



Scheme 23 Synthesis of 4'-fluoro-nucleosides by substitution of 4'-phenylsulfanyl developed by Kubota *et al.*<sup>91</sup>



Scheme 24 Synthesis of 4'-fluoro-nucleosides by radical dehydroxymethylative fluorination developed by Zhou *et al.*<sup>92</sup>

of 4-bromo-D-ribofuranose **317** with silver fluoride, afforded the L-lyxo-fluoride **319**. The correctly configured epimer **318**, was accessed from **317** after treatment with silver tetrafluoroborate, however only in a modest yield.

In another effort to circumvent generating 4'-fluoro epimers, Lee *et al.*, developed a strategy to access 4'-fluoro-nucleosides **325**–**327** involving a successive bromination-fluorination protocol using 1-O-acetyl-2,3,5-tri-O-benzoyl-β-D-ribose **320** as a substrate.<sup>70</sup> Reaction with *N*-bromosuccinimide (NBS) followed by treatment with boron trifluoride-etherate and silver fluoride (Scheme 22a) gave 4-fluoro-β-D-ribofuranose **321** which was then utilised in a modified Hilbert-Johnson *N*-glycosylation with adenine, cytosine or hypoxanthine to generate benzoyl protected derivatives **322**–**324**. Finally, deprotection with methanolic sodium carbonate gave 4'-fluoro-nucleosides **325**–**327** as illustrated in Scheme 22a. An alternative approach involving the NBS mediated bromination of 5-fluorouracil **328**, followed by fluorination gave **329** as illustrated in Scheme 22b. As before, deprotection with methanolic sodium carbonate was used to generate 4'-fluoro-5-fluorouracil **330**.<sup>70</sup>

Kubota *et al.*, developed a method for the synthesis of 4'-substituted cordycepin analogues. This involved the substitution of 4'-phenylsulfanyl as a leaving group from *N*<sup>6</sup>-pivaloylated **331**.<sup>91</sup> After reacting **331** with DAST/NBS in DCM, followed by

deprotection with NH<sub>3</sub>/MeOH, 4'-fluoro-cordycepin analogues **333** and **334** could be acquired as a mixture of diastereomers as illustrated in Scheme 23.

More recently Zhou *et al.*, developed a protocol for the synthesis of glycosyl fluorides, involving the silver promoted radical dehydroxymethylative fluorination of carbohydrates under mild conditions.<sup>92</sup> Mechanistically the reaction involves a radical fluorination *via* β-fragmentation of sugar-derived 5'-alkoxyl radical, and is conducted with Ag<sub>2</sub>CO<sub>3</sub> and Selectfluor in aqueous acetone. This method was used to access protected 4'-fluoro-uridine **337** in good yield, as illustrated in Scheme 24.

## Concluding remarks

It is perhaps surprising that 4'-fluoro-nucleosides have not had a more prominent focus in bioactives discovery, particularly so given that the natural product nucleocidin has been known for over 50 years. There has been a rich and diverse chemistry exploring 2'-fluoro and 3'-fluoro nucleosides, entities which have been ubiquitous in drug discovery and some have reaped large rewards as effective commercial products. The chemistry required to introduce fluorine into the 4'-position of nucleosides



is certainly more challenging, and perhaps the replacement of F for H in 4'-nucleosides has been viewed as a rather neutral modification relative to a much more proactive deoxyfluorination (F for OH) in 2'-fluoro and 3'-fluoro nucleotides. That said, the published and patented literature reviewed here indicate a recent and intensive interest in exploring 4'-fluoro-nucleosides, particularly in antiviral programmes, and we anticipate continued interest in this structural class. Elucidation of the enzymology involved in nucleocidin biosynthesis would further invigorate research into 4'-fluoro-nucleosides as it would offer a unique biotechnology, not available to other fluoro-nucleoside classes.

## Conflicts of interest

The authors have no conflicts to declare.

## Acknowledgements

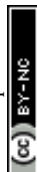
We thank EPSRC for a grant and the EU Horizon 2020 Sinfonia consortia for financial support.

## References

- N. A. Meanwell, *J. Med. Chem.*, 2018, **61**, 5822–5880.
- P. Jeschke, *Pest Manage. Sci.*, 2010, **66**, 10–27.
- P. Jeschke, *Pest Manage. Sci.*, 2017, **73**, 1053–1066.
- C. Isanbor and D. O'Hagan, *J. Fluor. Chem.*, 2006, **127**, 303–319.
- D. O'Hagan, *Chem. Soc. Rev.*, 2008, **37**, 308–319.
- R. Berger, G. Resnati, P. Metrangolo, E. Weber and J. Hulliger, *Chem. Soc. Rev.*, 2011, **40**, 3496–3508.
- T. Fujiwara and D. O'Hagan, *J. Fluor. Chem.*, 2014, **167**, 16–29.
- S. O. Thomas, V. L. Singleton, J. A. Lowery, R. W. Sharpe, L. M. Pruess, J. N. Porter, J. H. Mowat and N. Bohonos, *Ant. Ann.*, 1956, 716–721.
- A. Olszewska, R. Pohl and M. Hocek, *J. Org. Chem.*, 2017, **82**, 11431–11439.
- M. Chrominski, M. R. Baranowski, S. Chmielinski, J. Kowalska and J. Jemielity, *J. Org. Chem.*, 2020, **85**, 3440–3453.
- V. Kumar and E. Rozners, *ChemBioChem*, 2022, **23**, e202100560.
- F. Levi-Acobas, P. Rothlisberger, I. Sarac, P. Marliere, P. Herdewijn and M. Hollenstein, *ChemBioChem*, 2019, **20**, 3032–3040.
- A. E. Klopffer and J. W. Engels, *ChemBioChem*, 2004, **5**, 707–716.
- A. Istrate, M. Medvecky and C. J. Leumann, *Org. Lett.*, 2015, **17**, 1950–1953.
- S. Frei, A. Istrate and C. J. Leumann, *Beilstein J. Org. Chem.*, 2018, **14**, 3088–3097.
- R. El-Khoury and M. J. Damha, *Acc. Chem. Res.*, 2021, **54**, 2287–2297.
- M. Hollenstein and C. J. Leumann, *Org. Lett.*, 2003, **5**, 1987–1990.
- S. Ellipilli and K. N. Ganesh, *J. Org. Chem.*, 2015, **80**, 9185–9191.
- M. Luo, E. Groaz, G. Andrei, R. Snoeck, R. Kalker, R. G. Ptak, T. Hartman, R. W. Buckheit, D. Schols, S. De Jonghe and P. Herdewijn, *J. Med. Chem.*, 2017, **60**, 6220–6238.
- M. Luo, E. Groaz, R. Snoeck, G. Andrei and P. Herdewijn, *ACS Med. Chem. Lett.*, 2020, **11**, 1410–1415.
- P. Liu, A. Sharon and C. K. Chu, *J. Fluor. Chem.*, 2008, **129**, 743–766.
- K. W. Pankiewicz, *Carbohydr. Res.*, 2000, **327**, 87–105.
- L. Eyer, R. Nencka, E. de Clercq, K. Seley-Radtke and D. Růžek, *Antivir. Chem. Chemother.*, 2018, **26**, 2040206618761299.
- S. Pal, G. Chandra, S. Patel and S. Singh, *Chem. Rec.*, 2022, **22**, e2021003.
- D. R. Nelson, J. N. Cooper, J. P. Lalezari, E. Lawitz, P. J. Pockros, N. Gitlin, B. F. Freilich, Z. H. Younes, W. Harlan, R. Ghalib, G. Oguchi, P. J. Thuluvath, G. Ortiz-Lasanta, M. Rabinovitz, D. Berastein, M. Bennett, T. Hawkins, N. Ravendhran, A. M. Sheikh, P. Varunok, K. V. Kowdley, D. Hennicken, F. McPhee, I. Rana, E. A. Hughes and A.-S. Team, *Hepatology*, 2015, **61**, 1127–1135.
- J. S. Roth, H. Ford, M. Tanaka, H. Mitsuya and J. A. Kelley, *J. Chromatogr. B*, 1998, **712**, 199–210.
- L. W. Hertel, G. B. Boder, J. S. Kroin, S. M. Rinzel, G. A. Poore, G. C. Todd and G. B. Grindey, *Cancer Res.*, 1990, **50**, 4417–4422.
- P. Kozuch, N. Ibrahim, F. Khuri, P. Hoff, E. Estey, V. Gandhi, M. Du, M. B. Rios, W. Plunkett, M. J. Keating and H. Kantarjian, *Blood*, 1999, **94**, 127A–127A.
- N. Bhuma, S. S. Burade, A. V. Bagade, N. M. Kumbhar, K. M. Kodam and D. D. Dhavale, *Tetrahedron*, 2017, **73**, 6157–6163.
- J. B. Chang, *Acc. Chem. Res.*, 2022, **55**, 565–578.
- K. Detmer, D. Summerer and A. Marx, *Eur. J. Org. Chem.*, 2003, 1837–1846.
- D. Summerer and A. Marx, *J. Am. Chem. Soc.*, 2002, **124**, 910–911.
- M. Betson, N. Allanson and P. Wainwright, *Org. Biomol. Chem.*, 2014, **12**, 9291–9306.
- D. B. Smith, J. A. Martin, K. Klumpp, S. J. Baker, P. A. Blomgren, R. Devos, C. Granycome, J. Hang, C. J. Hobbs, W. R. Jiang, C. Laxton, S. Le Pogam, V. Leveque, H. Ma, G. Maile, J. H. Merrett, A. Pichota, K. Sarma, M. Smith, S. Swallow, J. Symons, D. Vesey, I. Najera and N. Cammack, *Bioorg. Med. Chem. Lett.*, 2007, **17**, 2570–2576.
- G. Y. Wang, N. Dyatkina, M. Prhac, C. Williams, V. Serebryany, Y. J. Hu, Y. F. Huang, J. Q. Wan, X. Y. Wu, J. Deval, A. Fung, Z. N. Jin, H. Fan, K. Shaw, H. Kang, Q. L. Zhang, Y. Tam, A. Stoycheva, A. Jekle, D. B. Smith and L. Beigelman, *J. Med. Chem.*, 2019, **62**, 4555–4570.
- T. Xu, C. Xu, D. Liu, J. Fan, Y. Pan, R. T. Li and X. Chen; *Int Patent Appl*, 2nd May, WO2019/080898A1, 2019.
- G. O. Morton, J. E. Lancaster, G. E. Vanlear, W. Fulmor and W. E. Meyer, *J. Am. Chem. Soc.*, 1969, **91**, 1535.
- C. W. Waller, J. B. Patrick, W. Fulmor and W. E. Meyer, *J. Am. Chem. Soc.*, 1957, **79**, 1011–1012.
- A. R. O. Pasternak, A. Bechthold and D. L. Zechel, *ChemBioChem*, 2022, **23**, e202200140.
- T. Awakawa, L. Barra and I. Abe, *J. Ind. Microbiol. Biotechnol.*, 2021, **48**, DOI: [10.1093/jimb/kuab001](https://doi.org/10.1093/jimb/kuab001).
- D. A. Shuman, M. J. Robins and R. K. Robins, *J. Am. Chem. Soc.*, 1970, **92**, 3434–3440.



- 42 I. D. Jenkins, J. P. H. Verheyden and J. G. Moffatt, *J. Am. Chem. Soc.*, 1976, **98**, 3346–3357.
- 43 J. R. Florini, Nucleocidin, in D. Gottlieb and P. D. Shaw ed., *Antibiotics, Mechanism of Action*, Springer-Verlag, New York, vol. 1, 1967, pp. 427–433.
- 44 C. W. Waller, P. W. Fryth, B. L. Hutchings and J. H. Williams, *J. Am. Chem. Soc.*, 1953, **75**, 2025.
- 45 E. J. Tobie, *J. Parasitol.*, 1957, **43**, 291–293.
- 46 L. E. Stephen and A. R. Gray, *J. Parasitol.*, 1960, **46**, 509–514.
- 47 C. J. Bacchi, C. Lambros, B. Goldberg, S. H. Hutner and G. D. Carvalho, *Antimicrob. Agents Chemother.*, 1974, **6**, 785–790.
- 48 J. R. Florini, H. H. Bird and P. H. Bell, *J. Biol. Chem.*, 1966, **241**, 1091–1098.
- 49 I. W. Sherman, *Comp. Biochem. Physiol., Part B: Biochem. Mol. Biol.*, 1976, **53**, 447–450.
- 50 J. Williamson and R. F. Macadam, *Trans. R. Soc. Trop. Med. Hyg.*, 1976, **70**, 130–137.
- 51 X. M. Zhu, S. Hackl, M. N. Thaker, L. Kalan, C. Weber, D. S. Urgast, E. M. Krupp, A. Brewer, S. Vanner, A. Szawiola, G. Yim, J. Feldmann, A. Bechthold, G. D. Wright and D. L. Zechel, *ChemBioChem*, 2015, **16**, 2498–2506.
- 52 S. Zhang, D. Klementz, J. Zhu, R. Makitrynssky, A. R. O. Pasternak, S. Gunther, D. L. Zechel and A. Bechtholda, *J. Biotechnol.*, 2019, **292**, 23–31.
- 53 X. Feng, N. Al Maharik, A. Bartholome, J. E. Janso, U. Reilly and D. O'Hagan, *Org. Biomol. Chem.*, 2017, **15**, 8006–8008.
- 54 U. Ngivprom, S. Kluaiphanngam, W. J. Ji, S. Siriwibool, A. Kamkaew, J. R. K. Cairns, Q. Zhang and R. Y. Lai, *RSC Adv.*, 2021, **11**, 3510–3515.
- 55 X. Feng, D. Bello, P. T. Lowe, J. Clark and D. O'Hagan, *Chem. Sci.*, 2019, **10**, 9501–9505.
- 56 Y. W. Chen, Q. Z. Zhang, X. Feng, M. Wojnowska and D. O'Hagan, *Org. Biomol. Chem.*, 2021, **19**, 10081–10084.
- 57 X. Feng, D. Bello and D. O'Hagan, *RSC Adv.*, 2021, **11**, 5291–5294.
- 58 F. Deleeuw and C. Altona, *Perkin Trans. 2*, 1982, 375–384.
- 59 C. Altona and M. Sundaralingam, *J. Am. Chem. Soc.*, 1973, **95**, 2333–2344.
- 60 T. Hakoshima, H. Omori, K. Tomita, H. Miki and M. Ikehara, *Nucleic Acids Res.*, 1981, **9**, 711–729.
- 61 M. N. Aher, N. D. Erande, V. A. Kumar, M. Fernandes and R. G. Gonnade, *Acta Crystallogr.*, 2020, **76**, 346.
- 62 T. Iimori, Y. Murai, Y. Wakizaka, Y. Ohtsuka, S. Ohuchi, Y. Kodama and T. Oishi, *Chem. Pharm. Bull.*, 1993, **41**, 775–777.
- 63 A. R. Maguire, W. D. Meng, S. M. Roberts and A. J. Willetts, *J. Chem. Soc., Perkin Trans. 1*, 1993, 1795–1808.
- 64 S. Martinez-Montero, G. F. Deleavey, A. Kulkarni, N. Martin-Pintado, P. Lindovska, M. Thomson, C. Gonzalez, M. Gotte and M. J. Damha, *J. Org. Chem.*, 2014, **79**, 5627–5635.
- 65 Y. F. Zhou, K. Lu, Q. Li, C. C. Fan and C. Z. Zhou, *Chem. – Eur. J.*, 2021, **27**, 14738–14746.
- 66 H. Shimada, K. Haraguchi, K. Hotta, T. Miyaike, Y. Kitagawa, H. Tanaka, R. Kaneda, H. Abe, S. Shuto, K. Mori, Y. Ueda, N. Kato, R. Snoeck, G. Andrei and J. Balzarini, *Bioorg. Med. Chem.*, 2014, **22**, 6174–6182.
- 67 I. D. Jenkins, J. P. Verheyden and J. G. Moffatt, *J. Am. Chem. Soc.*, 1971, **93**, 4323.
- 68 D. Guillermin, M. Muzard, B. Allart and G. Guillermin, *Bioorg. Med. Chem. Lett.*, 1995, **5**, 1455–1460.
- 69 B. A. Mayes, A. M. Moussa, A. J. Stewart and G. Gosselin, *Int. Patent*, Appl, 26th June, WO2014/099941A1, 2014.
- 70 S. Lee, C. Uttamapinant and G. L. Verdine, *Org. Lett.*, 2007, **9**, 5007–5009.
- 71 M. A. Ivanov, G. S. Ludva, A. V. Mukovnya, S. N. Kochetkov, V. L. Tunitskaya and L. A. Alexandrova, *Russ. J. Bioorg. Chem.*, 2010, **36**, 488–496.
- 72 T. Xu, C. Xu, D. Liu, J. Fan, Y. Pan, T. R. Li and X. Chen, *Int. Patent Appl.*, 26th June, WO2019/080898A1, 2014.
- 73 G. R. Owen, J. P. H. Verheyden and J. G. Moffatt, *J. Org. Chem.*, 1976, **41**, 3010–3017.
- 74 Q. Li, J. L. Chen, M. Trajkovski, Y. F. Zhou, C. C. Fan, K. Lu, P. P. Tang, X. C. Su, J. Plavec, Z. Xi and C. Z. Zhou, *J. Am. Chem. Soc.*, 2020, **142**, 4739–4748.
- 75 J. Sourimant, C. M. Lieber, M. Aggarwal, R. M. Cox, J. D. Wolf, J. J. Yoon, M. Toots, C. Ye, Z. Sticher, A. A. Kolykhalov, L. Martinez-Sobrido, G. R. Bluemling, M. G. Natchus, G. R. Painter and R. K. Plemper, *Science*, 2022, **375**, 161–167.
- 76 E. Malek-Adamian, M. B. Patrascu, S. K. Jana, S. Martinez-Montero, N. Moitessier and M. J. Damha, *J. Org. Chem.*, 2018, **83**, 9839–9849.
- 77 E. Malek-Adamian, J. Fakhoury, A. E. Arnold, S. Martinez-Montero, M. S. Shoichet and M. J. Damha, *Nucleic Acid Ther.*, 2019, **29**, 187–194.
- 78 S. Ajmera, A. R. Bapat, E. Stephanian and P. V. Danenberg, *J. Med. Chem.*, 1988, **31**, 1094–1098.
- 79 R. Abele, P. Alberto, S. Kaplan, P. Siegenthaler, V. Hofmann, H. J. Ryssel, D. Hartmann, E. E. Holdener and F. Cavalli, *J. Clin. Oncol.*, 1983, **1**, 750–754.
- 80 R. Abele, E. Kaplan, R. Grossenbacher, H. J. Schmid and F. Cavalli, *Eur. J. Cancer Clin. Oncol.*, 1984, **20**, 333–336.
- 81 T. Ishikawa, F. Sekiguchi, Y. Fukase, N. Sawada and H. Ishitsuka, *Cancer Res.*, 1998, **58**, 685–690.
- 82 S. Martinez-Montero, G. F. Deleavey, N. Martin-Pintado, J. F. Fakhoury, C. Gonzalez and M. J. Damha, *ACS Chem. Biol.*, 2015, **10**, 2016–2023.
- 83 L. K. McKenzie, R. El-Khoury, J. D. Thorpe, M. J. Damha and M. Hollenstein, *Chem. Soc. Rev.*, 2021, **50**, 5126–5164.
- 84 G. Wang, S. P. Lim, Y. L. Chen, J. Hunziker, R. Rao, F. Gu, C. C. Seh, N. A. Ghafar, H. Y. Xu, K. Chan, X. D. Lin, O. L. Saunders, M. Fenaux, W. D. Zhong, P. Y. Shi and F. Yokokawa, *Bioorg. Med. Chem. Lett.*, 2018, **28**, 2324–2327.
- 85 Z. H. Zheng, E. Groaz, R. Snoeck, S. De Jonghe, P. Herdewijn and G. Andrei, *ACS Med. Chem. Lett.*, 2021, **12**, 88–92.
- 86 S. Martinez-Montero, G. F. Deleavey, A. Dierker-Viik, P. Lindovska, T. Ilina, G. Portella, M. Orozco, M. A. Parniak, C. Gonzalez and M. J. Damha, *J. Org. Chem.*, 2015, **80**, 3083–3091.
- 87 G. Y. Wang, N. Dyatkina, M. Prhavc, C. Williams, V. Serebryany, Y. J. Hu, Y. F. Huang, X. Y. Wu, T. Q. Chen, W. S. Huang, V. K. Rajwanshi, J. Deval, A. Fung, Z. N. Jin, A. Stoycheva, K. Shaw, K. Gupta, Y. Tam, A. Jekle, D. B. Smith and L. Beigelman, *J. Med. Chem.*, 2020, **63**, 10380–10395.





- 88 G. Y. Wang, J. G. Wan, Y. J. Hu, X. Y. Wu, M. Prhac, N. Dyatkina, V. K. Rajwanshi, D. B. Smith, A. Jekle, A. Kinkade, J. A. Symons, Z. N. Jin, J. Deval, Q. L. Zhang, Y. Tam, S. Chanda, L. Blatt and L. Beigelman, *J. Med. Chem.*, 2016, **59**, 4611–4624.
- 89 L. Beigleman, J. Deval and M. Prhac; *Int Patent Appl*, 21st March, WO2019/053696A1, 2019.
- 90 R. J. Ferrier and S. R. Haines, *J. Chem. Soc., Perkin Trans. 1*, 1984, 1675–1681.
- 91 Y. Kubota, M. Ehara, K. Haraguchi and H. Tanaka, *J. Org. Chem.*, 2011, **76**, 8710–8717.
- 92 X. Zhou, H. Ding, P. W. Chen, L. Liu, Q. K. Sun, X. Y. Wang, P. Wang, Z. H. Lv and M. Li, *Angew. Chem., Int. Ed.*, 2020, **59**, 4138–4144.

